Chapter 5

The effect of plant fibres reinforcement on properties of oilseed meal based biocomposite films and biodegradable plates

5.1. Introduction

The economy of India contributes 17% to agriculture and 58% of Indian population depends on agriculture for their livelihood. The processing of marine food and agricultural feedstocks generates a lot of waste byproducts. The development of a biodegradable packaging material out of waste can provide us an opportunity to replace non-biodegradable petroleum-based plastics. Proteins, lipids, starches and their blends have been found to be runners in the production of biopolymeric film and biocomposites and also can resolve the problem they're of being biodegradable, disposal and sustainability on earth (Schettini et al., 2013).

As discussed in earlier chapters, the production of oilseed meals and plant fibres as by-products obtained in generous amount from food processing industries being wasted and creating pollution to the environment. The utilization of these by-products can be beneficial to both farmers and nation economy. The increment of awareness towards the environment and consumer demands needs to reduce the use of petroleum based plastics in food sectors. Our manufactured products must be sustainable and industrially eco-efficient has become an actual interest for upcoming generation. Burning this agricultural waste has become a serious issue in India as it generates air pollution thus contributing in global warming. Many creative approaches have been utilized by researchers to use trash produced by agricultural crops in an effort to lesson the deprivation of environment. One of the attempts is use of the fibres after extracting them from agro-waste into the development of natural polymers (Ravindran et al., 2019). Natural fibres are biodegradable, non-carcinogenic, inexpensive, posing no health risks, and easy to handle.

Fibrous plants are widely accessible in tropical countries, and some of them, like bananas, are used as agricultural crops. Banana bast fibre is a byproduct of growing banana plants. Better mechanical qualities may be obtained from the pseudo-stem of the banana plant by extracting a lingo-cellulosic fibre. Good specific strength qualities found in banana fibre are equivalent to those seen in traditional materials like glass fibre (Muralikrishna et al., 2020). Pseudo-stem of bananas fibres contains high levels of cellulose fibre. Coir fibre, a robust and resilient natural fibre found in coconut husk, is considered one of the toughest fibres in nature. Its chemical makeup has been previously studied and found to consist of cellulose, lignin, hemicellulose, extractives, and ash (Khalil et al., 2006). Coir fibre has a high cellulose content and it's a perfect starting point for the

creation of potentially high-value cellulose-based biomaterials (Rencoret et al., 2013). Sugarcane bagasse is a by-product of the sugar making process, and sugar mills' enormous stockpiles of sugarcane bagasse fibre provide them with an economic advantage over other fibres. The primary elements of sugarcane bagasse are cellulose, hemicellulose, lignin, ash, and wax. These chemical compositions of the sugarcane bagasse make it an excellent element for use as a reinforcing fibre in composite materials to create biomaterials with unique physical and chemical properties. The cellulose from sugarcane bagasse can improve the barrier properties and biocompatibility by reinforcing strength of such composite materials.

Usually polymer, glass, and metal-based containers are commonly used for the purpose of rigid packaging in the food industry. Moreover, the use of wood pulp as biodegradable packaging have a primary disadvantage i.e. it consumes a massive amount of energy to create the cardboards (Changmai and Badwaik, 2021). The main advantages of using plant fibre are renewability, high strength and elastic modulus, low density, non-abrasiveness and biodegradability. There is a growing trend to use such fibres as fillers and/or reinforcers in plastics composite (Teh et al., 2014; Koushki et al., 2015; Mohan et al., 2010). For the usage of biopolymeric films and natural composite packaging materials with improved mechanical properties are demanded in a wider range of applications. Since, the most of the biopolymeric films have low mechanical properties in comparison to petroleum-based plastics are well known, the additional use of plant fibres as fillers can be needful. The terms "biocomposites" refer to composite materials consisting of a bioplastic/biopolymeric and synthetic reinforcement, materials consisting of a synthetic plastic and natural reinforcement, or bioplastics reinforced with natural fillers or fibres. Biocompsites are lightweight and have advantageous mechanical qualities, cellulosic plant fibres have been one of the most popular natural fillers and reinforcements in polymer composites (Bátori, 2019). Scientists are working on development of new packaging materials by treating the fibres in various ways to increase their strength that can compete in the market with poly-oriented packaging materials and in their availability, quality and selection of any fibres, geographic location plays major role (Muneer et al., 2014).

Overall, there are five primary types of (bio)plastics-derived materials that are used to make disposable cutlery and utensils: (1) biodegradable and biobased; (2) non-biodegradable but biobased; (3) derived from non-renewable sources but biodegradable; (4) fossil-based and non-biodegradable; and (5) composites made of mixed miscellaneous

(bio)plastics that can also be combined with fillers of different origin (Dybka-Stępień et al., 2021). The use of biodegradable materials and their sphere of effect seem to be growing continuously (Mohareb and Mittal, 2007). Biodegradable plastics are found in nursery pots used in agriculture, foam packaging for industrial items, and fast-food flatware and food containers (Mohareb and Mittal, 2007). Moulded pulp products have been widely used in the disposable goods market because of its affordability, biodegradability, and ease of disposal. Moulded pulp products are replacing plastics in the food business as consumer expectations demand for sustainable and eco-friendly products (Zhang et al., 2022). The market for single-use cutlery and tableware may be divided into product categories such as straws, chopsticks, glasses, spoons, forks, sporks, cups, and so on (Dybka-Stępień et al., 2021).

Therefore, based on surveys on the previous reports of plant fibres (banana pseudo-stem, coconut coir and sugarcane bagasse), the present research work focuses on valorization of agro-waste by developing biocomposites and biodegradable plates. The study relies on the effective way in producing fibres and the detailed characterization of isolated fibres using various chemical, functional, physical, morphological and thermal properties. This comparative work can overlay the different fields of using plant fibres in future. The present study also includes the valorisation of agricultural by-products such as oilseed meals and plant fibres. Thus, the present study aims to develop and characterize biocomposites and biodegradable plates by direct utilization of oilseed meals and plant fibres. The study makes an effort to minimise any limitations related to the extraction of biomaterials and the synthesis of biocomposites and biodegradable plates.

5.2. Materials and Methods

5.2.1. Materials

The plant fibres of banana pseudo stem were collected within the campus of Tezpur University and the coconut coir, sugarcane bagasse, oilseed cakes (mustard, flaxseed and soybean seed) were collected from the vendors of Tezpur local market, Assam. The chemical used such as acacia gum, citric acid, glutaraldehyde and xanthan gum were procured from Hi Media Laboratories and Merck, India. The other chemical used in biocomposites development of laboratory grade such as glycerol, n-hexane and soy lecithin were ordered from Merck Chemicals, India. All chemicals used in this research were laboratory reagent grade compounds.

5.2.2. Methods

5.2.2.1. Oilseed sample preparation

The collected oilseed cakes were sorted manually, dried, grinded to turn into powder form. The oilseed cakes powder was sieved from 150 mesh and defatted with n-hexane (1:10 w/v) for 4 h. The defatted oilseed meals or powder were stored into a closed airtight container at 4˚ C for further use.

5.2.3. Pre-treatment of plant fibres

The raw fibres were pre-treated with alkaline solution as shown in Fig. 5.1. The banana fibres (500 g) were cut into small pieces and were immersed into 6% NaOH (v/v) solution overnight at room temperature. After the alkali treatment, the fibres were easily separated and washed under running water until pH turned to neutral. The fibres were filtered and dried at 70˚ C (Hariprasad et al., 2013). The coconut coir (200g) was sorted and soaked in 10% (w/v) NaOH solution for 3h at 70˚ C water bath with occasional stirring was followed by washing the fibres under running water multiple times to remove the soaked alkali until pH turned to neutral. The fibres were dried at 70˚ C (Rosa et al., 2010). The sugarcane bagasse (100g) was immersed into 10% (w/v) NaOH alkaline solution for 1h at room temperature under constant stirring. After the treatment, the fibres were sieved and washed into water neutral pH is maintained and was dried at 70˚ C (Bertoti et al., 2009). All the dried fibres were individually pulverized through dry and wet pulverizer (Model: LP 20, Make: Lincon, India) to decrease the size of the fibres, sieved (52 mesh) and stored in airtight containers for functional, morphological, physicochemical and thermal property analysis.

Fig. 5.1. Extraction of fibres from (a) raw banana pseudo-stem (b) raw coconut coir (c) raw sugarcane bagasse

5.4. Development of oilseed meals-gums crosslinked biocomposites incorporated with plant fibres

The composition of oilseed meals (mustard seed (20.50%): flaxseed (67.15%): soybean seed (12.33%), natural gums (0.5:1.5% w/w) and crosslinkers (10% w/w) were previously optimized for development of biopolymeric films were discussed in former chapters. The similar composition was used for the development of biocomposites with addition of plant fibres of banana pseudo-stem, coconut and sugarcane bagasse at 1, 2, 3, 4 & 5% w/w of oilseed meals shown in Table 5.1.

Solvent casting was used to create biocomposites based on oilseed meals natural gums. For the addition of the natural gums (Acacia & Xanthan powder) and crosslinkers (Citric acid), were priorly dissolved in 50 ml distilled water and heated at 80˚C for gelatinization on magnetic stirrer at 900 rpm (ABDOS MS H280 Pro, India) for 15 min. Separately, the known quantity of the oilseed meals along with Glycerol (75% w/w) as plasticiser is mixed separately in the rest 50 ml distilled water on magnetic stirrer at 900

rpm at 50˚C for 10 min. Afterwards, the natural gums crosslinkers suspension is gradually added into the oilseeds meal suspension with constant stirring at 900 rpm for uniform mixing for another 15 min at 50˚C. The entire mixture is heated to 90˚C for 30 min with occasional stirring, in a hot water bath (Modern, New Delhi), and then cooled in ice cold water. The suspension was mixed with 2% w/w soy lecithin, an emulsifier. Finally, the fibres of banana pseudo-stem, coconut and sugarcane bagasse with different percentage (1, 2, 3, 4 & 5% w/w) were incorporated into the final biocomposites suspension separately, stirred for 15 min at 0˚C. The biocomposites suspension was poured into petri plates after the air bubbles were removed by allowing the suspension to stay undisturbed for 10 minutes. To create uniform and smooth distribution, biocomposites petri dishes (150 x 25 mm size) were set with the support of a portable spirit level and dried in a hot air oven at 70˚C for 72 h. Following drying, the biocomposites were carefully removed from the petri plates, packed in ziplock pouches and placed inside the desiccator containing dried silica gel for further examination.

5.5. Development of biodegradable plates incorporated with plant fibres

The formulation of the biodegradable plates included the formulation of oilseed meals-gum and crosslinkers incorporated with plant fibres at 1, 2, 3, 4 & 5% as presented in Table 5.1. To manufacture plates, a dough was prepared. For this, the mixture was prepared in 2 stages. Formerly, a gel mixture was prepared with gums (acacia & xanthan), crosslinker (citric acid), plasticizer (glycerol 75% w/v) and emulsifier (soy lecithin 2% w/w) in 60 ml distilled water with 800 rpm (ABDOS MS H280 Pro, India) at 70 ºC until mixed evenly. Then, the gel mixture was added in dry mixture of oilseed meals and plant fibres (banana pseudo-stem, coconut coir and sugarcane bagasse).

The hot compression moulding machine (MAZORIA, TCB-1, baking machine, India) as shown in Fig. 5.2, with a circular double heat pan press coated with Teflon surfaces with 208 mm diameter and a 9 mm thickness was used in the formation of biodegradable plates (Marimuthu et al., 2024). The machine was pre-heat for 2 min at 100 ºC and greased with oil before use to avoid sticking. The homogeneous dough was formed and baked on hot compression machine at 170 ºC for 2 min to form sheets using manual hand pressing in such a way that the top pan mould was brought into contact with the bottom fixed pan and sealed tightly. After baking, the flattened baked sheets were removed from the machine. The final shape of the biodegradable plate was given by pressure

moulding of the flattened baked sheets in between two structured plates for 10 min and removed slowly. The biodegradable plates formed had diameter of 84 mm, thickness of 44.1 mm and height of approximately 21.2 mm. Following moulding, the plates were dried for an additional 30 min at 102 °C in a hot air oven (IGene Labserve Model No. IG-95HA0) to eliminate any remaining moisture. It was then cooled in a desiccator before being placed in a low-density polyethylene bag (LDPE) for storage for further analysis.

Fig. 5.2. Compression moulding machine

Table 5.1. Formulation of biocomposites and biodegradable plates incorporated with plant fibres

S.No.	Oilseed meals[a]	Natural gums[b]	Crosslinker[c]	Banana pseudostem[d]	Coconut coir[d]	Sugarcane Bagasse fibre[d]
1.				1%	1%	1%
2.	Mustard seed meal (20.50%),	Acacia Gum: Xanthan Gum (0.5:1.5% w/w of oilseed meal)	Citric acid (10% w/w of oilseed meal)	2%	2%	2%
3.	Flaxseed meal (67.15%),			3%	3%	3%
4.	Soybean seed meal (12.33%)			4%	4%	4%
5.				5%	5%	5%

[a] Oilseed meals of mustard, flaxseed and soybean ratio fixed as in pre-determined study for all the biocomposites
[b] Acacia gum and xanthan gum ratio 0.5:1.5% (w/w) of the oilseed meal sample is constant for all the biocomposites.
[c] Crosslinker (citric acid 10% w/w) represents the percentage addition of the citric acid with respect to the total amount of oilseed meals in 100 mL of biocomposites suspension is constant for all the biocomposites.
[d]BSF, CC & SBF (1-5%) represents the percentage addition of banana pseudostem, coconut coir & sugarcane bagasse fibre with respect to the total amount of oilseed meals in 100 mL of biocomposites suspension.

5.6. Characterization of plant fibres, biocomposites and biodegradable plates

The plant fibres and composites were analysed on the basis of physical, chemical, morphological, thermal, and functional aspects discussed in sections 5.6.1 to 5.6.22. The properties analysis of biodegradable plates was done based on physical (moisture content, thickness, water holding capacity, true density, contact angle, color, absorption rate, spreadability test), and mechanical analysis through compression test and biodegradability test discussed in section 5.6.23 to 5.6.27.

5.6.1. Cellulose, hemicellulose, lignin of plant fibres

The determination of cellulose, hemicellulose and lignin present in plant fibers were adapted as per literatures of Mansora et al., (2019); Stelmock et al., (1985). Van Soest's method is used to estimate the acid detergent fiber (ACF), neutral detergent fiber (NDF) and acid detergent lignin (ADL).

5.6.2. Ash content of plant fibres

The percentage ash present in the plant fibers were determined using the standard procedure described by Elaveniya and Jayamuthunagai, (2014). The plant fibre samples were ignited for three to four hours at 600°C in a muffle furnace to calculate the total ash concentration.

5.6.3. Bulk density of plant fibres

The bulk density is to analyze the loose or aerated property of the powder. A quantity of 2g sample powder was introduced in 10 ml measuring cylinder. The powder was slightly shaken to break any agglomerates if formed (Fazaeli et al., 2012). The volume was noted and calculated as in Eq. (5.1).

$$Bulk\ density\ (\frac{g}{ml}) = \frac{weight\ of\ the\ powder}{volume\ of\ the\ packing} \tag{5.1}$$

5.6.4. Tapped bulk density of plant fibres

For the tapped bulk density, 2 g of the powdered sample was taken in 10 ml measuring cylinder which was held in a vortex vibration for a minute. The volume of the sample was noted and measured in terms of 'g' per 'cm^3' according to the Eq. (5.2) (Manikantan et al., 2015):

$$Tapped\ bulk\ density\ (\frac{g}{cm3}) = \frac{weight\ of\ sample\ powder}{Tapped\ volume\ of\ packing} \tag{5.2}$$

5.6.5. True density of plant fibres

The true density works on displacement theorem. 5 g of the sample was taken in 25 ml measuring cylinder and toluene was used as displacement liquid. The final volume of the sample after displacement was observed and calculated as per Eq. (5.3) (Vishwakarma et al., 2012):

$$True\ density\ (\frac{g}{cm3}) = \frac{Mass\ of\ sample}{(volume\ of\ sample\ displaced - initial\ volume)} \tag{5.3}$$

5.6.6. Porosity of plant fibres

Porosity or bed porosity of the sample can be obtained mathematically based on prior calculated bulk density and tapped density as described by Madsen and Lilholt (2003) and porosity was calculated as shown in Eq. (5 4).

$$Porosity = 1 - \frac{Bulk\ density}{Tapped\ density} \qquad (5.4)$$

5.6.7. Particle size analysis of plant fibres

Dynamic Light Scattering (DLS) analysis is used to determine the particle size analysis of the plant fibres. The nano size of cellulose in natural fibre has been widely determined using DLS, also known as photon correlation spectroscopy, which is one of the best techniques for assessing nanosized particles. Measuring the random fluctuations in light intensity dispersed from a suspension or solution can provide an estimate of the particle size. The fiber's average particle size distribution was calculated using DLS (nanoplus-3). Analysis of the subsequent criteria was retained: dispersant name: water; viscosity (cP): 0.8872; temperature (°C): 25 °C; RI: 1.330 dispersant (Singha et al., 2023a).

5.6.8. Surface and pore size analysis of plant fibres

BET theory rationalizes the physical adsorption of gas molecules onto solid surfaces and underpins an analytical method for gauging the specific areas of materials. The instrument (Quantachrome Instrument; model NOVA 1000E, USA) uses nitrogen gas for adsorption–desorption method at 77 K. In order to remove all of the adsorbed water, the samples were degassed using thermal out-gassing for three hours at 100ºC. The Brunauer-Emmett-Teller (BET) and Barrett-Joyner-Halenda (BJH) techniques were utilized to compute the pore size distributions and specific surface values, respectively (Nascimento et al., 2022).

5.6.9. Water activity of plant fibres

The water activity measures the free moisture present on the surface of the material. The water activity of the plant fibers was measured using Aqua Lab 4TE dew point water activity meter (Decagon Devices, USA) with sensitivity ± 0.001 at 25 ºC according to literature of Veiga-Santos et al. (2005).

5.6.10. Oil and water absorption index of plant fibres

5g of the sample was mixed in 20ml distilled oil/water in centrifuge tube and allowed to stand at temperature at 30 ºC for 30 min. The tube with sample was agitated for 2 min before centrifuging at 4000 rpm for 20 min. The centrifuge tube containing the residual was reweighed after decanting and separating the supernatant. Water absorption

was estimated by determining the percent oil/water bound per gm powder (Omowaye-Taiwo et al., 2015). The oil/water absorption index was calculated as per Eq. (5.5).

$$Oil \ or \ Water \ absorption \ index \ (\%) = \frac{weight \ of \ sample \ residual}{weight \ of \ sample} \times 100 \qquad (5.5)$$

5.6.11. Oil and water swelling power of plant fibres

0.5 g of sample mixed with 20 ml of distilled water/oil was prepared and taken into conical flask. It was heated with water bath at 90 ºC with constant stirring for 30 min. After cooling, the sample was transferred into a pre-weighed centrifuged in room temperature (24 ºC) at 2200 rpm for 20 min. The supernatant was separated and the final weight of the centrifuge tube along with the residue was measured. The oil/water swelling power was calculated as per Eq. (5.6) (Aziz et al., 2011).

$$Oil \ or \ Water \ swelling \ index = \frac{weight \ of \ wel \ mass \ sediment \ (g)}{weight \ of \ dry \ matter \ in \ gel \ (g)} \qquad (5.6)$$

5.6.12. TEM of plant fibres

Transmission Electron Microscopy of plant fibers were analyzed at 200 kV applied voltage at 77K liquid Nitrogen through TEM instrument TECNAI G2 20 S-TWIN (200KV), USA; Resolution: 2.4A0. As described by Kumar et al., (2010), the fine powdered fiber samples were suspended in distilled water and sonicated in ultrasonic bath for 6 h to break the particles into more finer particles. A drop of the suspended particles with distilled water were placed on a fine-mesh carbon-coated TEM support grid and air dried and viewed under transmission electron microscope.

5.6.13. SEM of plant fibres and biocomposites

The sample's surface morphology was analyzed under JSM 6390LV scanning electron microscope (JEOL, Japan). Prior a thin layer of gold was coated on fine powdered fibres and the fibres were dried for 6 h at 60˚C before the analysis (Deepa et al., 2016).

5.6.14. DSC of plant fibres and biocomposites

In order to investigate the thermal properties of the sample, 0.01 g of the sample was sealed in a pan and put into a Differential scanning calorimetry (DSC) machine chamber. The sample was heated at a rate of 10.0 K/min from 20˚C to 300˚C using a Differential Scanning Calorimetry (214, Polyma, NETZSCH, Germany) (Zhang et al., 2018).

5.6.15. TGA of plant fibres and biocomposites

The TGA and DTG was analyzed in TGA instrument (TG 209 F1 LIBRA, NETZSCH, Germany) to study the degradation characteristics of the sample. The test was performed at temperature 25 ºC to 600 ºC with heating rate of 10 ºC/min in nitrogen gas with 3-5 mg fibre samples (Gond et al., 2021).

5.6.16. XRD of plant fibres and biocomposites

The material of the crystalline phase was identified through X-ray diffraction of the sample, and cell dimensions were measured. An X-ray diffractometer (BRUKER AXS D8 FOCUS) was used to analyse the sample. An X-ray beam operating at 100 mA and 50 kV was directed at the dried sample. The area of the crystalline and amorphous regions was determined using the 2 θ curve, which ranges from 10 to 80 degrees. The diffraction patterns were obtained using step scanning mode with 2θ = 5–60º, 5 s/step, and a step of 0.02º (Yumnam et al., 2023). The crystallinity degree was computed through the Eq. (5.7).

$$\text{Degree of crystallinity} = \frac{Area\ of\ crystalline\ peak}{Total\ area\ under\ curve\ (crystalline+amorphous)} \times 100 \qquad (5.7)$$

5.6.17. FTIR of plant fibres and biocomposites

The sample were subjected to infrared spectroscopy in order to determine the functional groups or chemicals compounds contained inside. The Bruker Equinox 55 spectrometer (Bruker Banner Lane, Conventry, Germany) was used to evaluate the biocomposites pallets using Fourier transform infrared spectroscopy in the 400–4000 cm^{-1} range (Singha et al., 2021).

5.6.18. Water solubility of biocomposites

The bio composite, measuring 2 by 2 cm, were dried at 105 ºC and then immersed in 40 ml of distilled water, maintaining room temperature throughout the day with frequent stirring. Subsequently, the damp samples were extracted from the water and subsequently dried in a hot air oven at 105 ºC for an additional 24 h. Calculations were made on the sample's solubility using Eq. (5.8) (Ojagh et al., 2010).

$$\text{Total soluble matter (\%)} = \frac{(initial\ dry\ weight - final\ dry\ weight)}{(initial\ dry\ weight)} \times 100 \qquad (5.8)$$

5.6.19. Mechanical properties of biocomposites

The textural and elongation property was determined as per methodology of Badwaik et al., (2014) using texture analyser (TA-HD Plus Stable microsystems, UK). The texture analyser tension mode was pre-set at pre-test speed (5 mm/s), test speed (1 mm/s), post-test speed (5 mm/s). The biocomposites was cut into 60×20 mm size pieces for measurement and placed in grip and load weighing 5 kg. The biocomposites were stretched upward until fallout. Each biocomposites sample was run in triplicate. After the experiment, the maximum force and the distance of the grips on curves was recorded for further calculation of the tensile strength and the elongation at break. The equation for the calculation of the mechanical properties is as given in Eq. (5.9) & (5.10).

$$Tensile\ strength\ (MPa) = \frac{Maximum\ force\ of\ the\ film\ (N)}{Cross\ sectional\ area\ of\ the\ film\ (m2)} \tag{5.9}$$

$$Elongation\ at\ break\ (\%) = \frac{Distance\ of\ rupture\ of\ film}{Onset\ distance\ of\ the\ separation\ of\ film} \times 100 \tag{5.10}$$

5.6.20. Water vapor permeability of biocomposites

The biocomposites were cut into 20×20 mm, fixed and sealed on glass beaker with round edges of diameter 50 mm partially filled with dried Silica crystals (0% Relative humidity). Then the sealed glass beaker with bio composite and silica was initially weighed and placed in desiccator filled with saturated K_2SO_4 solution of relative humidity of 97% and was placed in an incubator set at 25°C. The deviation in weight of biocomposites due to vapour exchange in desiccator was recorded for 7 days in every 24 h for the calculation of water vapour transmission rate (WVTR). The slope was calculated on weight change with function of time as linear regression (weight change vs time) and slope (g/h) divided by the biocomposites area given the value of water vapour transmission rate (Wu et al., 2013). The calculation of water vapour permeability was conducted using the Eq. (5.11).

$$WVP\ (g/Pa\ h\ m) = \frac{WVTR}{P(R1-R2)} \times X \tag{5.11}$$

Where, P = saturated vapor pressures of water (Pa) at room temperature

R1= relative humidity of the desiccator with K_2SO_4 solution

R2= relative humidity of the cup with dried Silica crystals

X = thickness of biocomposites (m) and the driving force in experimental conditions were taken as [P (R1 – R2)] is 3073.93 Pa.

5.6.21. Color of plant fibres, biocomposites and biodegradable plates

The color parameters of sample were calculated using Hunter Lab colorimeter (Ultrascan VIS, HunterLab. Inc., USA). The instrument was standardized using white and black tiles as Lightness L^* (L^*= 0 for black and L^*= 100 for white) and the color was recorded in reflectance of the sample. The recorded reading was analyzed in terms of chromaticity parameters a^* (green [-] to red [+]) and b^* (blue [-] to yellow [+]) (Teh et al., 2014). The whiteness index (WI) was measured using Eq. (5.12) (Lee et al., 2016).

$$WI = 100- [(100-L)^2 + a^2 + b^2]^{0.5}$$ (5.12)

5.6.22. Moisture content and thickness plant fibres, biocomposites and biodegradable plates

The moisture content of sample was determined by weight difference before and after drying in hot air oven at 105 ºC for 24h until a constant weight was obtained as described in Lee et al., (2005). The thickness of the biocomposites and biodegradable plates were analysed through micrometre at 3 random points (Alton M820–25, China) with a sensitivity of 0.01 mm (Pelissari et al., 2012).

5.6.23. Contact angle of biocomposites and biodegradable plates

The angle formed by the baseline of the drop and the tangent line at the point when the water droplet makes contact with the surface is known as the contact angle. The hydrophilic or hydrophobic characteristic of the biocomposite surface can be determined using the Water Contact Angle measurement (Pandey et al., 2020). The contact angle measurement was carried out using an Advanced Contact Angle Meter setup (Kyowa Interface Science VR, Japan). The biocomposites and biodegradable plates were cut into (2×2 cm) and using a syringe pump machine, the micro-droplets were created and then carefully placed on the cut samples. The subsequent water contact angles were calculated by the analysis of photographs taken at various positions on biocomposites surfaces using a white light source and a high-speed camera (Dubey and Mohanta, 2024).

5.6.24. Mechanical properties of biodegradable plates

The compression strength of the biodegradable plates were determined using P-75 compression platens probe by Texture Profile Analyser (TA-HD Plus Stable microsystems, UK). The biodegradable plates were turned upside down and the target strain of 10%, 30%,

50% and 70% were applied over the plates. The texture analyzer tension mode was set at 5 mm/sec pre-test speed, 1 mm/sec test speed, 5 mm/sec post-test speed, and 1 N trigger force with 100 kg load shell. The fracturability (N) and hardness (N) were determined from the graph plotted on force (N) variations as a function of distance (mm) (Changmai and Badwaik, 2021; Hazra and Sontakke, 2023).

5.6.25. Water holding capacity of biodegradable plates

The biodegradable plates were cut into 2×2 cm size and initial weight (W1) of the sample is weighed. Then, the samples were submerged in deionized water for a duration of 2 min. The final weight (W2) of the samples was weighed after removal of excess deionized water by filter paper from the surface of the sample (Changmai and Badwaik, 2021). The weight gained from water absorption was calculated using Eq. (5.13).

$$Water\ holding\ capacity\ (\%) = \frac{(W2-W1)}{W1} \times 100 \qquad (5.13)$$

5.6.26. Spreadability of biodegradable plates

This test is performed according to method of Rana et al., (2023) with little changes to determine the maximum amount of time the biodegradable plates can brace water before outflow. It is a crucial way of determining plate performance in the presence of food. Five different food model (water, oil, syrup, honey and ketchup) variants were filled into the plates and checked every 5 min for leakage for 15 min at room temperature. The analysis were performed in triplicate.

5.6.27. Biodegradability test of biodegradable plates

The soil biodegradability test was analyzed as per the procedure of Changmai and Badwaik, (2021). The biodegradable plates were cut, and initial weight (W1) of the plate pieces was recorded. The sample pieces were then buried under 5 cm deep in pots filled with soil. The pots were incubated under room temperature for one month. The pot's soil was sprayed with water at regular intervals. The plate pieces were removed from the soil at 5 days interval, washed, dried and weight (W2) was noted. By tracking weight variations as a function of burial time, biodegradation was calculated. Lastly, using eq. (5.14), the weight loss of the container components was calculated.

$$Weight\ loss\ (\%) = \frac{(W1-W2)}{W1} \times 100 \qquad (5.14)$$

5.6.28. Statistical Analysis

The plant fibres, biocomposites, biodegradable plates properties were examined using IBM SPSS Statistics 23 software. The mean differences of the biocomposites and biodegradable plates were compared using analysis of variance. The mean values of the plant fibres, biocomposites and biodegradable plates parameters were compared using Duncan's Multiple Range Test ($p < 0.05$).

5.7. Results and Discussion

The result and discussion have been discussed in the following text into two sections (a) characterization the properties of plant fibres (banana pseudostem, coconut coir & sugarcane bagasse) and its effects on the developed biocomposite films (b) development and characterization of biodegradable plates.

5.7.1. Characterization of plant fibers (banana pseudostem, coconut coir and sugarcane bagasse)

5.7.1.1. Cellulose, hemicellulose, lignin

The cellulose content in the plant fibers contributes maximum percentage in comparison to hemicellulose and lignin percentage. The percentage of cellulose content was found highest in banana pseudo-stem fibers and lowest in coconut coir. The presence of cellulose in banana pseudo-stem fibers, coconut coir and sugarcane bagasse fibers were found as 60.28%, 22.42% and 47.39% respectively (Table 5.2). The percentage of hemicellulose was found to be the highest in sugarcane bagasse and the lowest in coconut coir. The hemicellulose present in banana pseudo-stem fibers, coconut coir and sugarcane bagasse fibers were 12.32%, 7.74% and 30.37% respectively (Table 5.2). The role of lignin in fibers behaves as binder for cellulose and as energy storage system. The percentage lignin was recorded in banana pseudo-stem fibers, coconut coir and sugarcane bagasse fibers as 17.38%, 17.32% and 9.56% respectively. The lignin content was found to be the highest in banana pseudo-stem fibers and the lowest in coconut coir. Similar study was reported by Gond et al. (2021) for sugarcane bagasse contains hemicellulose (20–25%), cellulose (45–55%) & lignin (18–24%). The banana pseudo-stem contains cellulose 63–64%, hemicellulose 10% and 5% lignin as reported in literatures of Millogo et al. (2015).

The coconut coir contains cellulose 31.27%, hemicellulose 14.98% and lignin 15.07% as reported in literatures of Mukhopadhyay et al. (2008).

5.7.1.2. Ash content

Ash content calculation provides the amount of mineral content present in the plant fibers which were recorded as 2.23%, 1.20% and 0.72% in banana pseudo-stem fibers, coconut coir and sugarcane bagasse fibers respectively (Table 5.2). The ash content was found to be the highest in banana pseudo-stem and the lowest in sugarcane bagasse fibers. Similar ash content was observed in literatures of Aziz et al., (2011); Gond et al., (2021); Mukhopadhyay et al., (2008), the sugarcane bagasse, coconut coir & banana pseudostem fibre contains (1– 4%), 8.65% and 3.03 % ash content respectively.

Table 5.2. Chemical properties of banana pseudo-stem, coconut coir & sugarcane bagasse fibres

S. No.	Fibers	Cellulose (%)	Hemicellulose (%)	Lignin (%)	Ash (%)
1.	Banana pseudo-stem	60.28 ± 2.31^c	12.32 ± 0.84^b	17.38 ± 0.07^b	2.23 ± 0.05^c
2.	Coconut coir	22.42 ± 1.06^a	7.74 ± 0.36^a	17.32 ± 0.02^b	1.20 ± 0.01^b
3.	Sugarcane bagasse	47.39 ± 3.03^b	30.37 ± 2.21^c	9.56 ± 0.07^a	0.72 ± 0.03^a

All the mentioned values are means of three replicates ± standard deviation. The letters superscripted as a, b & c on the values shows significant differences ($p< 0.05$).

5.7.1.3. Moisture content

Reduced moisture content have the potential to extend shelf life by inhibiting microbial development and spoilage (Leang and Saw, 2011). The moisture content was found highest in coconut coir and lowest in sugarcane bagasse fibers. The amount of moisture present in banana pseudo-stem fibers, coconut coir and sugarcane bagasse fibers were 6.15±0.03%, 8.88±0.52% and 2.05±0.07% respectively (Table 5.3). It was reported that banana pseudo-stem fibres, coconut coir and sugarcane bagasse have 8.57%, 10.10%, 9.21% moisture content in literature of Ewansiha et al., (2012); Guimarães et al., (2009).

5.7.1.4. Bulk density

Bulk density of the plant fibers is presented in Table 5.3. The bulk density of banana pseudo-stem fibers, coconut coir and sugarcane bagasse fibers were recorded as 0.14 ± 0.006, 0.05 ± 0.001 and 0.11 ± 0.003 g/cm^3 respectively. Banana pseudo-stem fibers had the highest bulk density and was found lowest in coconut coir. The density of banana pseudo-stem fibres ranged between 0.95–1.35 g/cm^3, coconut coir in range of 1.15-1.32 g/cm^3 and sugarcane fibres had 1.25 g/cm^3 was reported in literature of Gond et al., (2021); Kumar and Raja, (2021); Mishra and Basu, (2020).

5.7.1.5. Tapped density

The values of tapped density were found highest in banana pseudo-stem fibers with 0.20 ± 0.02 g/cm^3 and was found lowest in coconut coir with 0.07 ± 0.00 g/cm^3 (Table 5.3). Sugarcane bagasse fibers had tapped density 0.15 ± 0.01 g/cm^3. Similar study was recorded for coconut coir as 0.12 g/cm^3 (Gichuki et al., 2022), banana pseudo-stem as 1400 kg/m^3 (Arifuzzaman Khan et al., 2013) and sugarcane bagasse as 0.15 g/cm^3 (Fauziyah and Yuwono, 2021).

5.7.1.6. True density

The values of true density were recorded in ranges of 0.09 to 1.67 g/cm^3 as shown in Table 5.3. Sugarcane bagasse fibers obtained the highest true density with 1.67 g/cm^3 whereas, coconut coir had lowest true density as 0.09 g/cm^3. Banana pseudo-stem fibers obtained true density with 1.33 g/cm^3. Similarly, true density was observed in sugarcane bagasse 1.331 g/cm^3 (De Lange et al., 2014), coconut coir as 1.42 g/cm^3 (Mishra et al., 2017).

5.7.1.7. Porosity

The values of porosity of banana pseudo-stem fibers, coconut coir and sugarcane bagasse fibers were recorded as 0.29, 0.31 and 0.24 respectively. The porosity of the coconut coir was found highest whereas sugarcane bagasse fibers had the lowest porosity (Table 5.3). Results obtained in literatures for porosity of banana pseudo-stem are 8.46 (Jahanzeb et al., 2022) and porosity of light and dark wood was 0.80 and 0.82 respectively (Lal, 2017).

5.7.1.8. Water activity

The water activity of the plant fibers ranged from 0.80 to 0.86. The water activity was found highest in coconut coir with 0.86 and was found lowest in banana pseudo-stem fibers with 0.80. Sugarcane bagasse fiber had water activity of 0.81 (Table 5.3). Similar results obtained for water activity of pineapple pomace was 0.14 (Selani et al., 2014) and that of banana peel dietary fibre concentrate was banana peel dietary fibre concentrate was 0.43-0.53 (Wachirasiri et al., 2009). The water activity of the blanched and unblanched banana pseudostem fibres ranging from 0.35-0.51 was also noted in Ma (2015).

Table 5.3. Physical properties of banana pseudo-stem, coconut coir & sugarcane bagasse fibres

S.No.	Fibers	Moisture content (%)	Loose bulk density (g/cm³)	Tapped bulk density (g/cm³)	True density (g/cm³)	Porosity	Water activity
1.	Banana pseudo-stem	6.15 ± 0.03^b	0.14 ± 0.006^c	0.20 ± 0.02^c	1.33 ± 0.47^b	0.29 ± 0.04^a	0.80 ± 0.02^a
2.	Coconut coir	8.88 ± 0.52^c	0.05 ± 0.001^a	0.07 ± 0.00^a	0.09 ± 0.00^a	0.31 ± 0.01^a	0.86 ± 0.02^b
3.	Sugarcane bagasse	2.05 ± 0.07^a	0.11 ± 0.003^b	0.15 ± 0.01^b	1.67 ± 0.47^b	0.24 ± 0.04^a	0.81 ± 0.01^a

All the mentioned values are means of three replicates ± standard deviation. The letters superscripted as a, b & c on the values shows significant differences ($p < 0.05$).

5.7.1.9. Particle size analysis

DLS helps in studying the particle distribution of the fibers in an aqueous by evaluating the hydrodynamic diameter of the particle in the suspension. The average particle size of the banana pseudo-stem fibers, coconut coir and sugarcane bagasse fibers were 12.8 nm, 46,962.8 nm and 6,893.5 nm respectively. The analysis of particle size distribution is shown in Fig. 5.3. Sugarcane bagasse nanocellulose average particle size was reported in range of 18.17- 220 nm by literatures of Gond et al., (2021); Mandal and

Chakrabarty, (2011). Coconut coir fibre with average particle size of 35.5 to 262.4 nm was reported in Sujatha et al., (2024) whereas banana pseudo-stem fibre average size value in range of 4–100 nm was noted by Abraham et al., (2013).
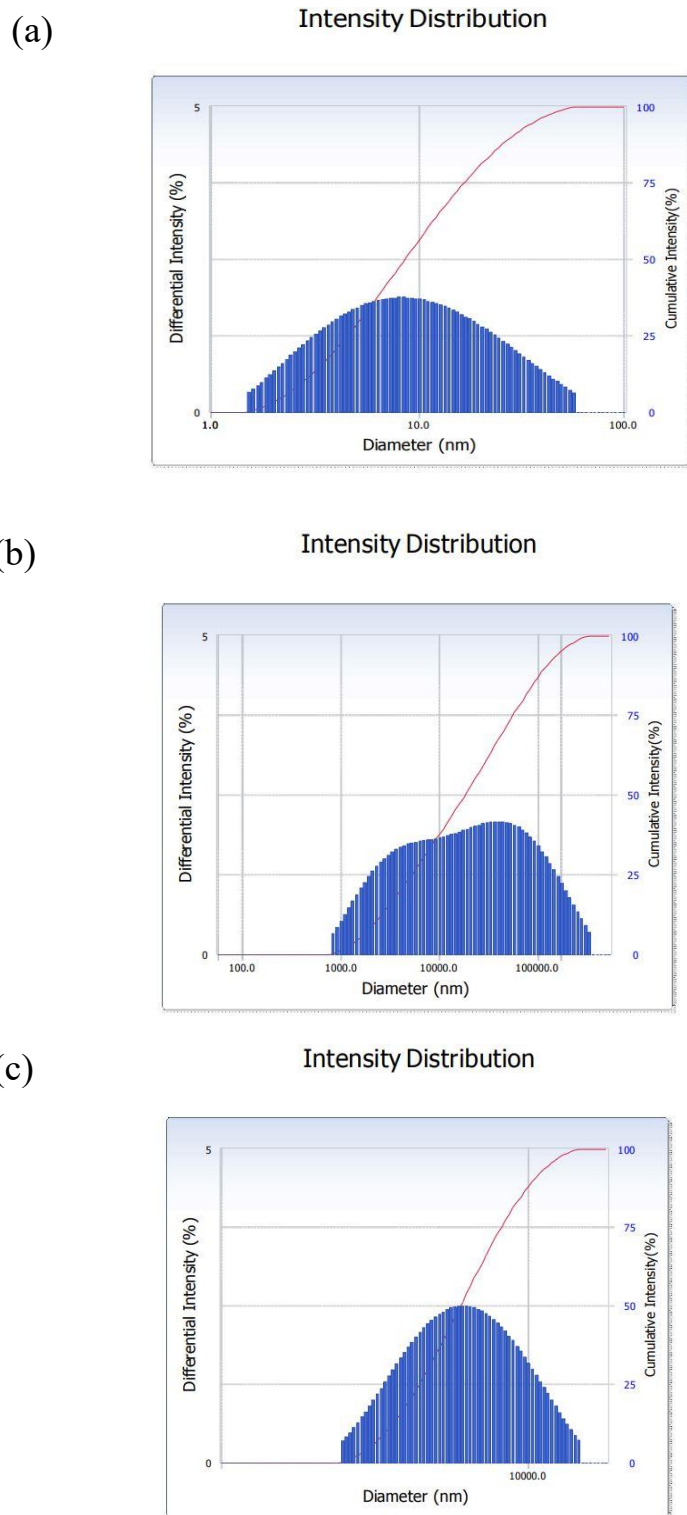
(a)

(b)

(c)

Fig. 5.3. Intensity distribution of the (a) banana pseudo-stem (b) coconut coir (c) sugarcane bagasse plant fibres fibers

5.7.1.10. Surface and pore size analysis

The specific surface area and porosity of the produced samples are determined by N_2 adsorption–desorption isotherm analysis (Begum et al., 2015). Fig. 5.4 shows the N_2 adsorption-desorption isotherm and Table 5.4 displays the pore structure parameters such as pore volume, pore radius, pore surface area obtained by BJH, and BET surface area obtained by BET-BJH methods for banana pseudo-stem, coconut coir & sugarcane bagasse fibres. There are three different sizes of particle pores: macropores ($\geq$50 nm), mesopores (2-4 nm), and micropores ($\leq$2 nm) (Maseko et al., 2021).

The BET surface area of the banana pseudo-stem, coconut coir & sugarcane bagasse fibres are found to be 3.865 m²/g, 1.195 m²/g and 0.761 m²/g, respectively. The results of pore diameter of the plant fibres (banana pseudo-stem, coconut coir & sugarcane bagasse fibres) were determined as 2.897 nm, 4.583 nm and 2.924 nm respectively. The structural parameters of plant fibres (banana pseudo-stem, coconut coir & sugarcane bagasse fibres) such as pore volume as 0.003 cm^3 g^{-1}, 0.001 cm^3 g^{-1} and 0.001 cm^3 g^{-1} were recorded in corresponding to pore surface area as 2.180 m^2 g^{-1}, 1.014 m^2 g^{-1} and 0.224 m^2 g^{-1} respectively. Similar study was conducted on crude and modified coconut coir having pore radius was noted as 1.64 nm and 2.10 nm respectively (Nascimento et al., 2022). BET-BJH study on kapok fibre pore volume had 1.94 cm^3 g^{-1} and D_{BJH} with 2.29 nm (An et al., 2019). Banana fibre had total pore volume of 0.81 cm^3/g (Sivadas et al., 2019).
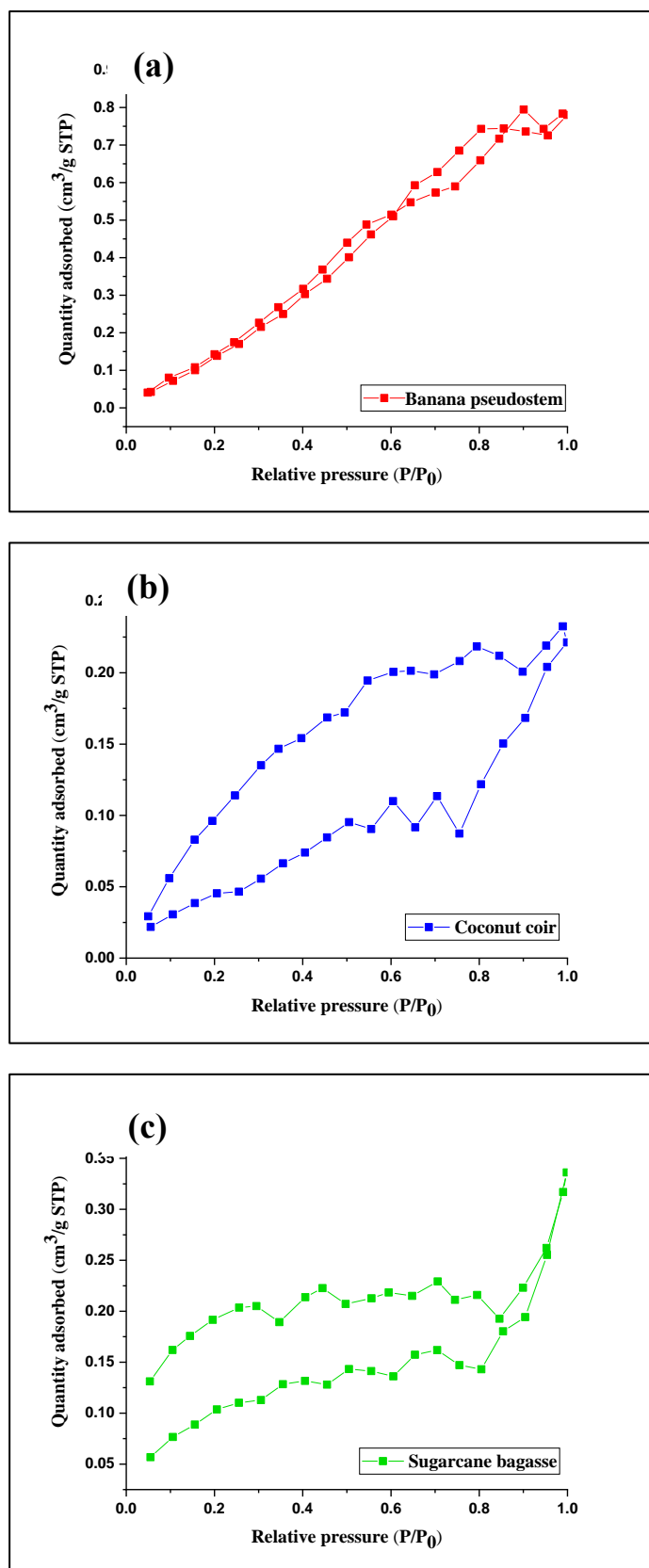
Fig. 5.4. BET N$_2$ adsorption–desorption isotherms of (a) banana pseudo-stem (b) coconut coir (c) sugarcane bagasse fibres

Table 5.4. Pore structure parameters obtained by BET and BJH methods for banana pseudo-stem, coconut coir & sugarcane bagasse fibres

Parameters	Banana pseudo-stem	Coconut coir	Sugarcane bagasse
BET data			
Surface area (m^2 g^{-1})	3.865	1.195	0.761
BJH data			
Pore volume (cm^3 g^{-1})	0.003	0.001	0.001
Pore radius (nm)	1.7023	2.141	1.710
Pore surface area (m^2 g^{-1})	2.180	1.014	0.224

5.7.1.11. Color analysis

The color analysis of the plant fibers is presented in Table 5.5. The color values obtained through the Hunter Lab colorimeter were conducted in respect to L*, a*, b*, and whiteness index. The whiteness index (WI) values obtained ranged in between 42.11 to 48.26. The WI found highest in banana pseudo-stem fibers and lowest in coconut coir. The L* values of banana pseudo-stem fibers, coconut coir and sugarcane bagasse fibers were 56.36, 49.27 and 64.30 respectively. The a* values of banana pseudo-stem fibers, coconut coir and sugarcane bagasse fibers were 3.96, 5.85 and 3.20 respectively. And b* values of banana pseudo-stem fibers, coconut coir and sugarcane bagasse fibers were 13.90, 10.91 & 16.63 respectively. Similar studies were reported in Balakrishnan et al., (2020). The L*, a* & b* values of the banana pseudostems fibres were higher and the color of the fibres were lighter in color than those in the present study. Whereas, the L*, a* & b* values for sugarcane bagasse matched with the values recorded with untreated sugarcane bagasse fibres in study of Lam et al., 2017. The dark color of coconut fibres was explained by a study conducted on cellulose extraction from matured coconut coir had darker color in compared to young coir. The lignin content of mature coconut coir is usually higher, giving the cellulose fibres a brownish or yellowish hue (Klunklin et al., 2023).

Table 5.5. Color analysis of banana pseudo-stem, coconut coir and sugarcane bagasse fibres

S.No.	Fibres	L*	a*	b*	Whiteness Index
1.	Banana pseudo-stem	56.36±3.05[ab]	3.96±0.52[a]	13.90±1.43[ab]	48.26
2.	Coconut coir	49.27±1.08[a]	5.85±0.33[b]	10.91±0.71[a]	42.11
3.	Sugarcane bagasse	64.30±7.57[b]	3.20±0.60[a]	16.63±2.16[b]	42.79

All the mentioned values are means of three replicates ± standard deviation. The letters superscripted as a, b & c on the values shows significant differences ($p < 0.05$).

5.7.1.12. Oil and water absorption index

There was no significant difference ($p \leq 0.05$) observed in the values of oil and water absorption index of the plant fibers. The oil absorption index ranged from 6.22% to 7.54% and water absorption index ranged from 12.54% to 13.02%. The banana pseudo-stem fibers have the highest oil absorption index but the lowest water absorption index whereas, sugarcane bagasse fibers had the lowest oil absorption index but highest water absorption index as discussed in Table 5.6. Water holding capacity of coconut fibre as 4.4 g water/g, 7.5 g water/g for sugarcane bagasse and banana pseudostem flour is 10.7 g water/g was observed in Ma, J. (2015) whereas, the oil holding capacity of pineapple pomace was 2.10 g oil/g sample in literatures of Selani et al., (2014) and banana peel dietary fibre concentrate was 4.75 g oil/g fibre in literature of Wachirasiri et al., (2009).

5.7.1.13. Oil and water swelling power

The oil and water swelling power are shown in Table 5.6. The values of oil swelling power of plant fibers ranged from 5.62-10.87 whereas, the water swelling power of the plant fibers ranged from 12.59- 14.62. Oil swelling power was found highest in coconut coir and lowest in sugarcane bagasse fibers whereas, water swelling power was found highest in sugarcane bagasse fibers and lowest in coconut coir (Table 3). The water swelling capacity of microcrystalline cellulose from coir fibers was reported as 8.5 g/g sample (Gichuki et al., 2022) and transverse swelling of coconut fibre in water as 5-15% (Mishra and Basu, 2020). Native banana pseudo-stem flour swelling power was noted as 9.48 g of swollen granules/g of dry matter in literature of Aziz et al., (2011).

Table 5.6. Physical properties of banana pseudo-stem, coconut coir and sugarcane bagasse fibres

S.No.	Fibres	Water absorption index (%)	Oil absorption index (%)	Water swelling power (g)	Oil swelling power (g)
1.	Banana pseudo-stem	12.54 ± 0.71^a	7.54 ± 0.91^a	14.62 ± 0.58^b	8.23 ± 0.34^{ab}
2.	Coconut coir	12.54 ± 0.11^a	6.47 ± 0.05^a	12.59 ± 0.36^a	10.87 ± 2.27^b
3.	Sugarcane bagasse	13.02 ± 0.58^a	6.22 ± 0.30^a	14.12 ± 0.62^b	5.62 ± 0.56^a

All the mentioned values are means of three replicates ± standard deviation. The letters superscripted as a, b & c on the values shows significant differences ($p < 0.05$).

5.7.1.14. SEM

Scanning Electron Microscopy (SEM) of the plant fibers are presented in Fig. 5.5. In Fig. 5.5 (a), 5.5 (b) and 5.5 (c) presenting banana pseudo-stem fibers, coconut coir and sugarcane bagasse fibers shows that none of the fibers have smooth surface. Even the structure of the fiber surface varied. The particles visualizing nearby the main large fibers can be the broken particles of hemicellulose and lignin in all the fibers images. Sugarcane bagasse have cylindrical, sharp edges, cracks and broken particles nearby in the fiber particles can be easily seen in the SEM images (Hussain et al., 2022). Banana pseudo-stem fibers are also small, cylindrical and thicker in length. The cracks and sharpness in the fibre structure were lesser than sugarcane bagasse fibres. Certain vegetative materials adhere to the rough surface of physically removed fibres. The physical extraction process leaves behind an uneven surface that is covered in encrusting materials such as pectin, lignin, and hemicellulose (Jayaprabha et al., 2011). Coconut coir have long cylindrical structure with less breakage and lesser damaged structure than the other fibers. The outer layers of the fibre are dissolved or degraded by the NaOH treatment, which results in a finer surface texture. Mature coir's fibres typically have a higher degree of lignification, giving the material a harder, more rigid structure. Therefore, some lignin and other contaminants are visible in mature coconut coir (Klunklin et al., 2023).
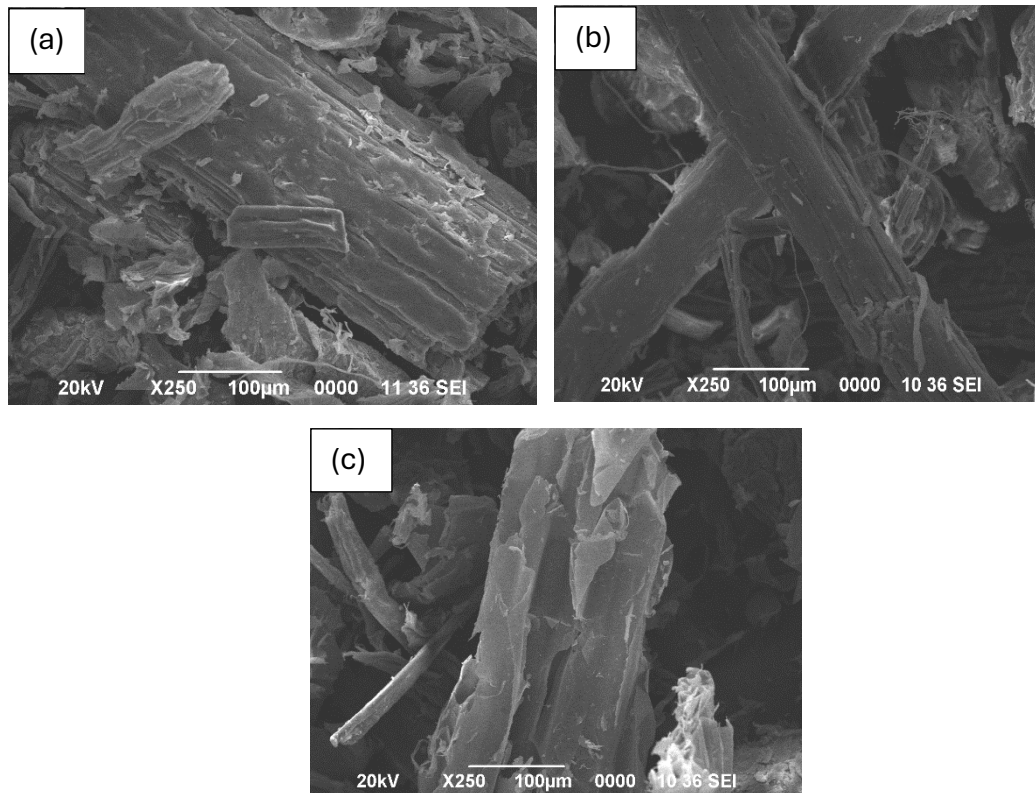
Fig. 5.5. SEM micrographs of (a) banana pseudo-stem (b) coconut coir (c) sugarcane bagasse plant fibres fibers

5.7.1.15. TEM

Transmission electron microscopy (TEM) of the plant fibers is presented in Fig. 5.6. TEM was used to determine the nano structure of the fibre (Merais et al., 2022). Fig. 5.6 (a), (b) and (c) show the banana pseudo-stem fibers, coconut coir and sugarcane bagasse fibers respectively. The TEM pictures were produced following a 30-minute high-intensity ultrasonication treatment. The figures show all the fibers at 0.2 μm, with different and unique structures. Sugarcane bagasse fibers have no sharp edges in TEM analysis and each fiber particle is evenly distributed having thinner fiber strands (Merais et al., 2022) whereas, coconut coir uneven distribution of the particles of variant sizes. The dark spots in between the fibres can be have heavy particles of coconut outer shell in shape of nanorods separating and dispersing in water (Nang An et al., 2020). The fibers of banana show a network of lengthy, intertwined cellulose filaments made up the nano fibrils can be seen in the images. The nanofibres after homogeneity develop a web-like form (Merais et al., 2022).

(a)

(b)

(c)
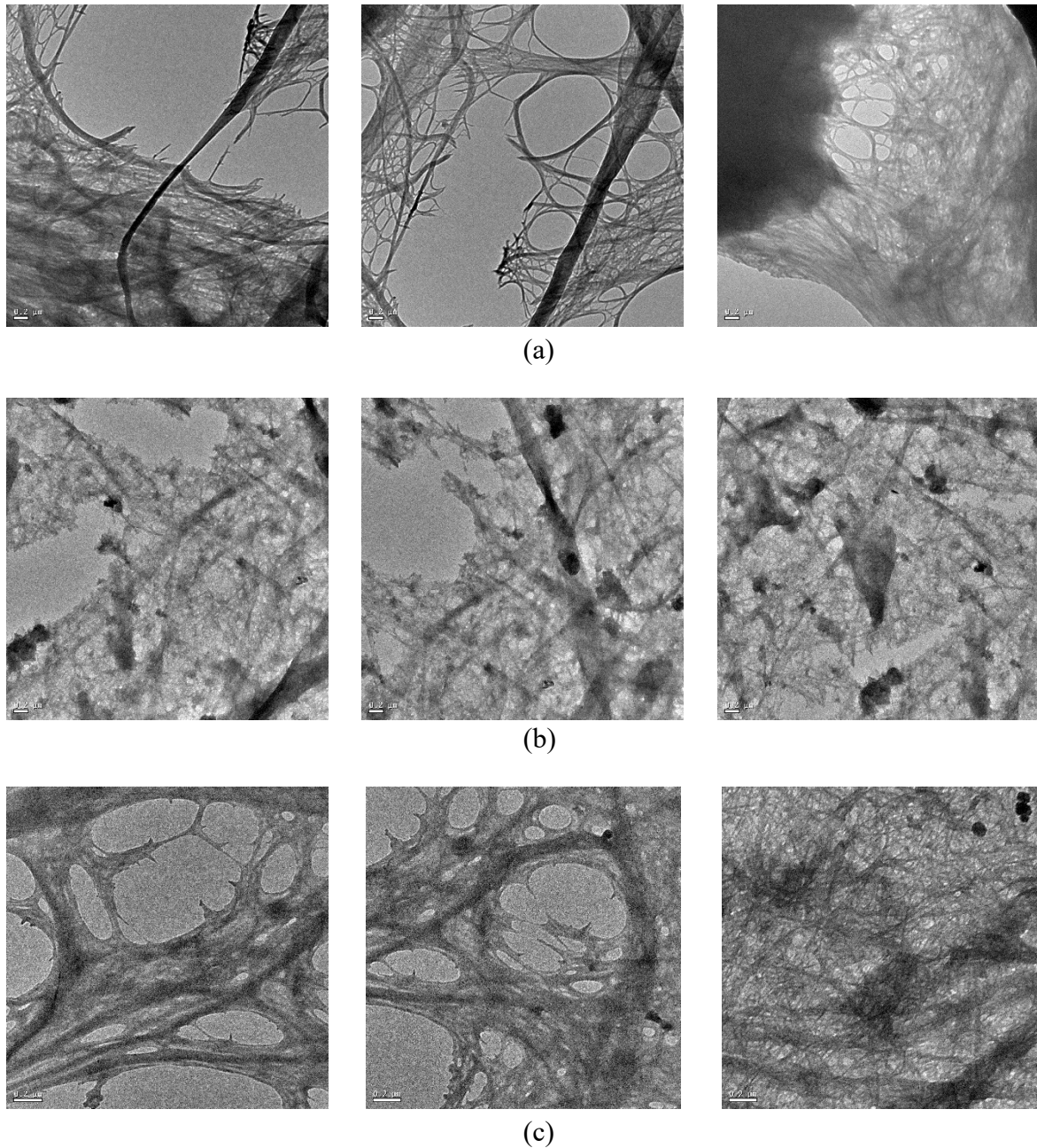
Fig. 5.6. TEM analysis of (a) banana pseudo-stem (b) coconut coir (c) sugarcane bagasse plant fibres fibers under 0.2 µm

5.7.1.16. TGA and DSC

The thermal stability of the plant fibers was determined through Thermogravimetric analysis at temperature range of 25 ºC to 600 ºC in nitrogen gas at the rate of 10K/min. Thermal degradation generally occurs in three stages i.e. evaporation of moisture from the fibers, degradation of hemicellulose and decomposition of cellulose and lignin (Asim et al., 2020). Fig. 5.7 represents the TGA analysis of the banana pseudo-stem fibers, coconut coir and sugarcane bagasse fibers. During the first stage of degradation, the

moisture content evaporation occurs at temperature range of 40-177 ºC for banana pseudo-stem fibers, 35-216ºC for coconut coir and 37-101ºC for sugarcane bagasse fibers (Essabir et al., 2016; Merais et al., 2022). The weight loss of the sample for banana pseudo-stem fibers, coconut coir and sugarcane bagasse fibers were 1.34%, 9.09% and 8.36% respectively. While the heating continues, the volatile components releases and hemicellulose and pectin in the plant fibers degrades along with decrease in weight of the fiber sample. In the second stage of degradation, the range of temperature for banana pseudo-stem, coconut, sugarcane fibers were recorded at 202 ºC, 225-343 ºC and 211-356 ºC respectively (Abraham et al., 2013; Pereira et al., 2011). The amount of weight loss in the sample were 4.08%, 48.64% and 48.33% for banana pseudo-stem, coconut, sugarcane fibers respectively. In the third or in some cases the forth stages of degradation, the toughest substances of the plant fibers degradations occurs i.e., cellulose and lignin. The temperature range recorded for banana pseudo-stem, coconut, sugarcane fibers were at 333 ºC, 357-600 ºC and 365-600 ºC respectively (Hosokawa et al., 2016). The weight loss for banana pseudo-stem, coconut, sugarcane fibers were observed as 1.37%, 12.89% and 14.97% respectively.
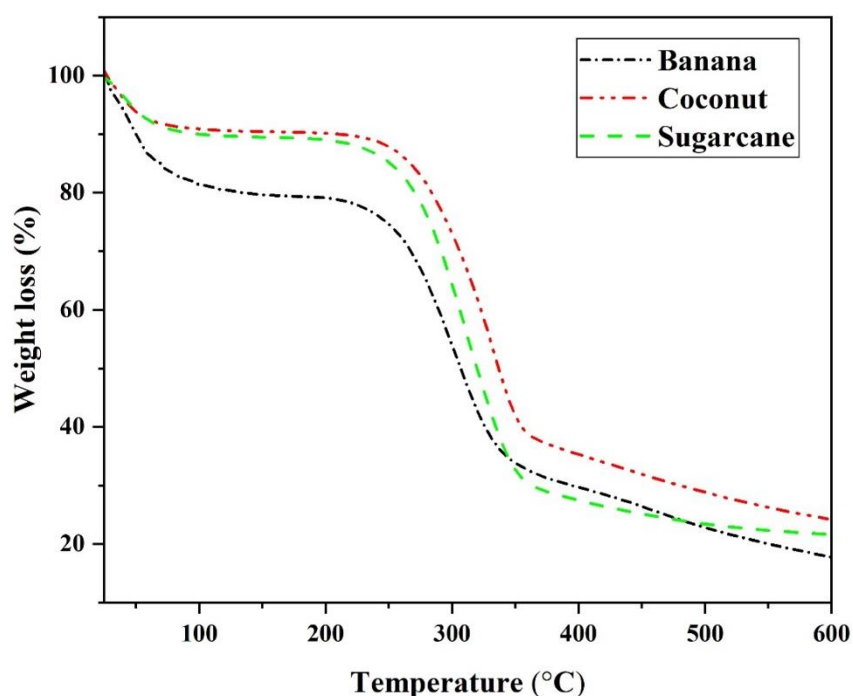

Fig. 5.7. TGA of (a) banana pseudo-stem (b) coconut coir (c) sugarcane bagasse fibres

Moreover, to support the above TGA explanation, the differential scanning calorimetry thermogram for plant fibers is presented in Table 5.7 As observed in Fig. 5.8 , the initial peaks at 34.2ºC, 32.1ºC and 31.9ºC presents the moisture evaporation from the fibers of banana pseudo-stem, coconut and sugarcane bagasse respectively (Pereira et al., 2014). The shape endotherm peaks obtained in all the three plant fibers at 67.2ºC, 71.4ºC and 73.3ºC show the degradation of hemicellulose and volatile elements present in the fibers similarly described in TGA thermographs (Guimarães et al., 2009). The enthalpy obtained of the fibers of banana pseudo-stem, coconut and sugarcane bagasse were 216.8, 127.7 and 158.2 J/g respectively. There was also presence of 2nd endothermic peak observed in DSC thermographs of plant fibers in range of 257-360ºC in banana pseudo-stem, 242-343ºC in coconut coir and 215-304ºC in sugarcane bagasse describes the decomposition of cellulose and lignin as discussed in TGA graphs (Fig. 5) (Pereira et al., 2014, 2011).
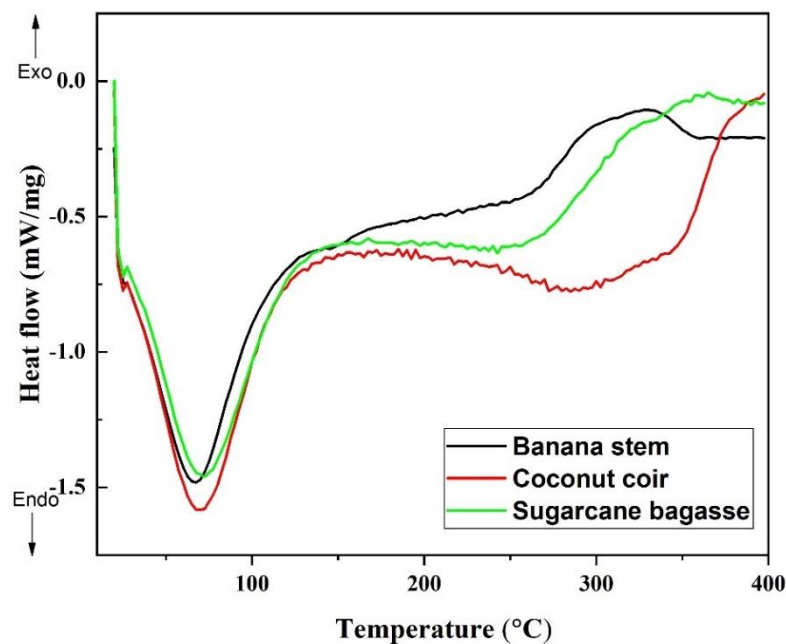
Fig. 5.8. DSC of (a) banana pseudo-stem (b) coconut coir (c) sugarcane bagasse fibres

Table 5.7. DSC analysis of banana pseudo-stem, coconut coir and sugarcane bagasse fibres

Fibres	Temperature range (⁰)		Maxima peak (⁰)	Enthalpy (J/g)
	T_o	T_e	T_m	ΔH_m
Banana pseudo-stem	34.2	99.9	67.2	216.8
Coconut coir	32.1	113.9	71.4	127.7
Sugarcane bagasse	31.9	126.4	73.3	158.2

5.7.1.17. XRD

X-ray Diffraction analysis of the plant fibers are presented in Fig. 5.9. The XRD is used to analyze the crystallinity or amorphous state of the fiber sample. The major peaks obtained in banana pseudo-stem fibers were 22.26º, 15.55º and 35.18º. Most crystalline peaks of banana variety (*Musa balbisiana*) were in the range of 13 - 25° and 32.5 – 40° with semi-crystalline peaks Ma, J. (2015). These peaks are associated to the salts of inorganic components, like potassium, chloride, calcium, and phosphor, as detected in X-ray fluorescence (Pereira et al., 2014). The major peaks obtained of Coconut coir peaks were at 14.50º, 22.16º and 35.02º whereas, the major peaks obtained for sugarcane bagasse fibers were at 15.54º, 22.23º and 34.51º The percentage crystallinity recorded for banana pseudo-stem fibers, coconut coir and sugarcane bagasse fibers were 40.48%, 35.50% and 5.93% respectively. The broad peaks is thought to be the overlapped peak of two peaks at 20.1º and 21.9º as well as the peak of amorphous cellulose at 17.3º. This suggests that type I cellulose was converted into type II cellulose and numerous amorphous cellulose structures following ionic liquid dissolution and regeneration (Abraham et al., 2013; Ai et al., 2021; Gilfillan et al., 2014).
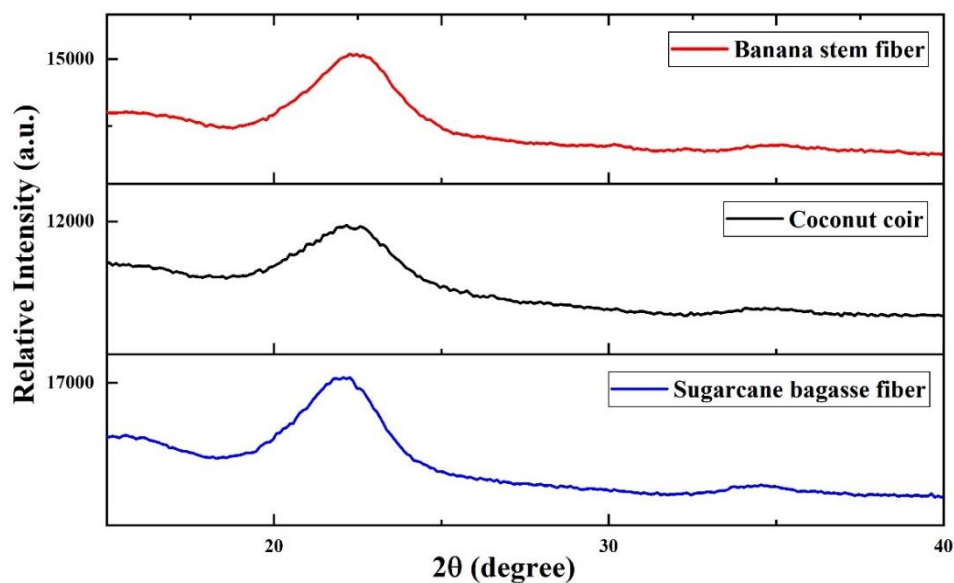
Fig. 5.9. XRD of (a) banana pseudo-stem (b) coconut coir (c) sugarcane bagasse fibres

5.7.1.18. FTIR

The Fourier-transform infrared spectroscopy of the plant fibers are presented in Fig. 5.10. The appearance of characteristic absorption peaks are due to the presence of functional groups present in the plant fibers such as cellulose, hemicellulose, lignin, pectin, moisture content, other volatile compounds etc. The FTIR analysis was carried out in range of 400-4000 cm^{-1}. Some of the common peaks attained in all three plant fibers were 3435, 2924, 1634, 1163, 1051 and 896 cm^{-1}. The peaks under 3200-3850 cm^{-1} are considered as O-H groups of cellulose. 2924 cm^{-1} peaks and nearby are considered as C-H group stretching vibrations. 1634 cm^{-1} peaks shows the presence of bound moisture content as asymmetric stretching vibration of carboxylate formed after oxidation of O-H bending. The peaks at 1163 cm^{-1} shows the presence of C-O-C glycosidic linkages with high content of hemicellulose and cellulose. The peaks at 1051 cm^{-1} depict a strong S=O stretching of sulfoxide, C-O stretching of primary alcohol and CO-O-CO stretching aldehydes. The small, sharp peaks at 896 cm^{-1} and nearby indicate cellulose, glycosidic C-H deformation with ring vibration, and O-H bending. There was also presence of sharp peaks at 1511 cm^{-1} absorptions associated to ring stretching vibrations of C=C as aromatic nature of lignin and methyl pectin in fibers of coconut coir and banana pseudo-stems but seems to dissolve in sugarcane bagasse fibers (Divyashree et al., 2016; Fitch-Vargas et al., 2019; Gond et al.,

2021; Gupta et al., 2020; Kumar and Raja, 2021; Li et al., 2015; Mandal and Chakrabarty, 2011; Pereira et al., 2014; Rosa et al., 2010; Simão et al., 2016; Wu et al., 2019).
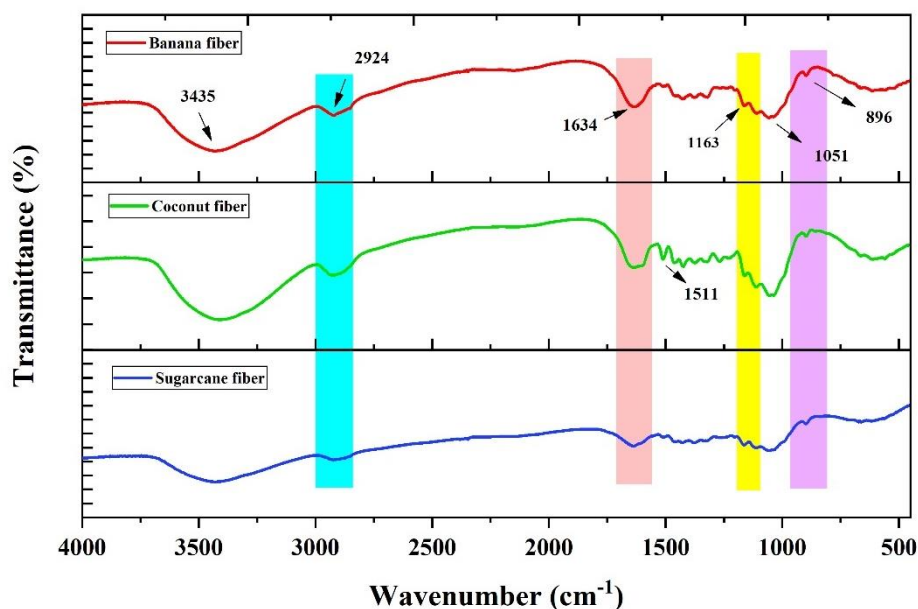

Fig. 5.10. FTIR of (a) banana pseudo-stem (b) coconut coir (c) sugarcane bagasse fibres

5.7.2. Characterization of biocomposites added with plant fibres

5.7.2.1. Thickness and moisture content

The biocomposites incorporated with plant fibres had thickness range from 0.55 to 0.57 mm. Similar thickness was reported by Annandarajah et al., (2018); Singha et al., (2023b). Thickness is an important parameter to study the other beneficial properties of the biocomposites such as mechanical, barrier properties although maintaining the thickness made from natural sources for commercial basis is still a challenge (Alves Lopes et al., 2020). There was significant difference ($p \leq 0.5$) between the values of thickness of biocomposites. The thickness of the biocomposites increased with addition in percentage of the fibres (Table 5.8).

The moisture content of the biocomposites ranged from 30.74 to 31.38% in banana fibre-added composite, 32.07 to 34.41% in coconut coir-added composite and 24.82 to 32.18% in sugarcane bagasse fibre added composite. The moisture content was found the highest in 1% coconut coir added composite with 34.41% and was found the lowest in 5% sugarcane bagasse fibre added composite with 24.82% (Table 5.8). The moisture content

was reported to decrease with addition of plant fibres in the biocomposites. This decrease can be attributed to hydrophobic nature of lignin present in the fibres (Plengnok and Jarukumjorn, 2020). Similar report was observed in characterization of biopolymer films of alginate and babassu coconut mesocarp (Lopes et al., 2020) and in sugarcane bagasse fibre on the properties of sweet lime peel and polyvinyl alcohol-based biodegradable films (Singha et al., 2023a). There was significant difference ($p \leq 0.5$) found in moisture content of the biocomposites.

5.7.2.2. Water solubility

The water solubility determines the weight loss and degradation process when disposed of into water of the composite when subjected to occasional agitation for a specific time. The water solubility (Table 5.8) of the composite added was plant fibres tends to increase with addition in percentage of plant fibres (Singha et al., 2023b). The water solubility of the biocomposites was studied by keeping the composite into distilled water for 24 h. The solubility of the banana fibres added with biocomposites had solubility range 35.45 to 37.98% whereas, the biocomposites added with coconut coir and sugarcane bagasse fibres had 40.67 to 45.06% and 35.06 to 45.12% respectively. The least solubility was found in 1% sugarcane bagasse added composite with 35.06% and was found highest in composite added with 5% sugarcane bagasse fibres 45.12%. The water solubility of the biocomposites was seen to increase significantly with addition of plant fibres. Since the bound matrix particles starts to loose from fibres as it swells in high amount of water. Addition of plant fibres increases the hydroxyl groups of nanocellulose increase the H-bonding to react with water thus, the protein tend to solubilize in water (Sukyai et al., 2018).

5.7.2.3. Tensile strength

The tensile strength determines the study of the mechanical properties of the biocomposites. The banana fibres 5% added composite had highest tensile strength with 1.74 MPa and the lowest tensile strength with 0.83 MPa was found in 1% sugarcane bagasse fibre composite. The range of tensile strength for banana fibre, coconut coir and sugarcane bagasse composite were 1.17 to 1.96 MPa, 0.91 to 1.30 MPa and 0.83 to 1.28 MPa respectively (Table 5.8). The tensile strength increased with the addition of plant fibres in the biocomposites. Although the composite appears brittle, it does not affect the mechanical strength of the composite. Similar observation wsas reported by Patel and

Joshi, (2020), who found that the tensile strength increased, as the concentration of banana nanocellulose fibres was added but further addition of nanofibres resulted in decrease in tensile strength due to suspended nanoparticles made the composite brittle in texture. Previous researchers Jagadeesan et al., (2023) found similar finding that addition of fillers more than 10%, due to lack of sufficient matrix to connect the matrix to the reinforcement, resulted in a reduction in tensile strength, and as the content of the reinforcement increased, the content of the matrix decreased for the development of sesame oil cake cellulose micro-fillers reinforced with basalt/banana fibre-based hybrid polymeric composite.

5.7.2.4. Elongation at break

The mechanical property i.e., elongation at break is analyzed through Texture analyser. This property is inversely proportional to tensile strength. The highest elongation at break was found in coconut coir enforced biocomposites with 9.69% and the lowest percent elongation was found in 5% coconut coir enforced biocomposites with 5.61%. The range of percent elongation for banana fibre, coconut coir and sugarcane bagasse composite were 7.11 to 9.14%, 5.61 to 9.69% and 6.19 to 8.89% respectively. As seen in Table 5.8, as tensile strength of the biocomposites incorporated with plant fibres, the percentage elongation decreases (Wu et al., 2019). Similar study was reported by Joshi, (2020), where the addition of nanocellulose of banana plant fibres into a polyvinyl alcohol to prepare a composite found the tensile increases and then decreases as composite becomes brittle. This exceptional result also affects the elongation of composite as well portraying that though the strength of the biocomposites decreases with increase in addition to nanocellulose, the elongation of the biocomposites increases and vice versa.

5.7.2.5. Water vapor permeability

The water vapor permeability gives the barrier property of biocomposites. The water vapor permeability was found the lowest in 1% sugarcane bagasse fibre enforced composites with 4.55 $gs^{-1}m^{-1}Pa^{-1}$. The water vapor permeability was found the highest in 5% banana fibre enforced biocomposite with 6.25 $gs^{-1}m^{-1}Pa^{-1}$. The water vapor permeability ranges from 5.16 to 6.25 $gs^{-1}m^{-1}Pa^{-1}$, 4.88 to 5.37 $gs^{-1}m^{-1}Pa^{-1}$ and 4.55 to 5.56 $gs^{-1}m^{-1}Pa^{-1}$ for banana fibre, coconut coir and sugarcane bagasse fibre enforced biocomposites (Table 5.8). The values of water vapor permeability increased with the addition of plant fibres in the composite. Also, the plant fibres such as banana pseudo-stem contains calcium crystals which develop micro-pores that elongates during process of

biocomposites drying and produce voids and gaps as observed in the morphological analysis in the biocomposites interrupting bonding of fibres in matrix and prompt the exchange gas and water vapors (Faradilla et al., 2018). This similar behaviour was observed in Alves et al., (2020) when studying the water vapor permeability of composites formed by babassu coconut mesocarp, alginate and glycerol with 5.153 decreased to 3.615 g.mm/m^2.day.kPa after second stage treatment of the films in aqueous Ca^{2+} solution.

Table 5.8. Properties of biocomposites incorporated with plant fibres

Fibres biocomposites	Moisture content (%)	Thickness (mm)	Solubility (%)	Tensile Strength (MPa)	Elongation at Break (%)	Water vapor Permeability×10^{-10} (gs^{-1}m^{-1}Pa^{-1})
OGCF 10%	30.98±1.00	0.55±0.01	35.83±0.37	1.15±0.30	10.68±0.83	3.8±0.010
Banana pseudostem 1%	31.38±0.18[de]	0.55±0.06[a]	35.45±0.21[a]	1.17±0.12[a]	9.14±0.43[abc]	5.16
Banana pseudostem 2%	31.20±0.26[cde]	0.56±0.03[b]	36.18±0.02[b]	1.22±0.19[ab]	9.11±2.74[bc]	5.25
Banana pseudostem 3%	31.11±0.35[cde]	0.56±0.03[b]	37.68±0.18[c]	1.22±0.39[ab]	9.01±1.38[abc]	5.35
Banana pseudostem 4%	30.87±0.26[cd]	0.57±0.03[c]	37.31±0.09[c]	1.74±0.33[b]	7.51±1.10[bc]	5.69
Banana pseudostem 5%	30.74±0.23[c]	0.57±0.04[c]	37.98±0.01[c]	1.96±0.0[a]	7.11±1.26[abc]	6.25
Coconut coir 1%	34.41±0.26[i]	0.55±0.04[a]	40.67±0.05[e]	0.91±0.23[a]	9.69±2.78[abc]	4.88
Coconut coir 2%	33.73±0.15[h]	0.55±0.03a	43.55±0.03[f]	0.95±0.13[a]	7.14±0.24[a]	4.92
Coconut coir 3%	32.11±0.22[fg]	0.56±0.03[b]	44.22±0.02[g]	0.96±0.26[a]	7.09±0.46[c]	5.30

Coconut coir 4%	32.07 ± 0.32^{fg}	0.56 ± 0.05^{b}	44.95 ± 0.02^{g}	1.11 ± 0.36^{a}	6.89 ± 1.72^{abc}	5.36
Coconut coir 5%	32.07 ± 0.32^{fg}	0.57 ± 0.06^{c}	45.06 ± 0.02^{h}	1.30 ± 0.23^{ab}	5.61 ± 0.77^{abc}	5.37
Sugarcane bagasse 1%	32.18 ± 0.34^{g}	0.55 ± 0.02^{a}	35.06 ± 0.04^{a}	0.83 ± 0.12^{a}	8.89 ± 1.06^{abc}	4.55
Sugarcane bagasse 2%	31.62 ± 0.16^{ef}	0.56 ± 0.03^{b}	35.19 ± 0.02^{a}	0.91 ± 0.18^{a}	8.56 ± 0.94^{abc}	4.88
Sugarcane bagasse 3%	29.67 ± 0.17^{b}	0.57 ± 0.03^{c}	36.71 ± 0.02^{b}	1.12 ± 0.16^{a}	7.59 ± 1.96^{abc}	5.16
Sugarcane bagasse 4%	29.50 ± 0.19^{b}	0.57 ± 0.04^{c}	38.45 ± 0.03^{d}	1.15 ± 0.17^{a}	7.59 ± 0.96^{ab}	5.24
Sugarcane bagasse 5%	24.82 ± 0.17^{a}	0.57 ± 0.02^{c}	45.12 ± 0.21^{h}	1.28 ± 0.43^{ab}	6.19 ± 0.16^{abc}	5.56

OGCF= oilseed meals-gum crosslinked biopolymeric film without plant fibres. All the mentioned values are means of three replicates ± standard deviation. The letters superscripted as a, b, c & d on the values shows significant differences (p < 0.05).

5.7.2.6. Color and whiteness index

The color analysis and whiteness index of the biocomposites added with plant fibres were measured through Hunter Lab colorimeter. The color analysis results of banana fibres, coconut coir and sugarcane bagasse fibres reinforced biocomposites were procured with respect to L*, a* and b* and whiteness index. There was no significant difference was found in the color of coconut fibre added composite, but significant difference (p≤0.5) was found in the composite of banana fibres and coconut coir added composite as shown in Table 5.9. The L* values ranged from 24.90- 27.06 for banana, 25.13- 25.82 for coconut and 23.67- 26.24 for sugarcane bagasse fibre added composite. All the values for a* and b* were found positive indicating the color of composite were reddish yellow in color. The darkness color in the composite were due to the raw agricultural materials of oilseed meals and plant fibres used as base for film production (Oliveira et al., 2015).

The whiteness index was found highest in 2% banana fibre added biocomposites with 22.61 and lowest in 2% sugarcane bagasse fibre added composite (Table 5.9). The value of L*, a* and b* was found highest in 1% banana pseudostem biocomposites with 27.06, 5% coconut coir biocomposites with 4.60 and 1% banana fibre biocomposites with 6.42 respectively. The value of L* was found lowest in 2% sugarcane bagasse fibre

123

biocomposites with 23.67 and the lowest value of a* and b* was found in 3% banana pseudostem biocomposites with 1.22 and 1.22 respectively. There were noticeable results of color analysis after addition of plant fibres at different concentration to influence the color of biocomposites. The color of composite gets darker as the concentration of plant fibres increases due to lignin and natural pigments in raw materials (Otenda et al., 2022; Oliveira et al., 2015). The L* values decrease from 27.06 to 24.90 in banana pseudostems based composites. Similar case was observed in the coconut coir and sugarcane bagasse fibre-based biocomposites.

Table 5.9. Color and Whiteness Index of biocomposites incorporated with plant fibres

Fibres biocomposites	L*	a*	b*	WI
Banana pseudostem 1%	27.06±0.17[b]	3.37±0.34[cd]	6.42±0.51[c]	22.50
Banana pseudostem 2%	27.03±3.17[b]	2.06±0.96[abc]	3.11±2.40[ab]	22.61
Banana pseudostem 3%	24.90±0.27[ab]	1.22±0.09[a]	1.22±0.05[a]	20.93
Banana pseudostem 4%	26.48±2.47[ab]	2.20±0.87[abc]	2.99±2.08[ab]	22.16
Banana pseudostem 5%	25.82±0.87[ab]	1.74±0.54[ab]	2.52±1.40[ab]	21.63
Coconut coir 1%	25.71±0.49[ab]	1.78±0.07[ab]	1.78±0.18[ab]	21.55
Coconut coir 2%	25.70±0.09[ab]	2.50±0.06[abcd]	2.08±0.26[ab]	21.53
Coconut coir 3%	25.37±0.07[ab]	2.03±0.34[abc]	1.93±0.32[ab]	21.28
Coconut coir 4%	25.13±0.07[ab]	2.83±0.69[bcd]	2.74±0.48[ab]	21.08
Coconut coir 5%	25.95±0.32[ab]	4.60±0.45[e]	4.12±1.39[bc]	21.65
Sugarcane bagasse 1%	26.24±2.59[ab]	2.71±0.98[bcd]	3.57±2.32[ab]	21.96
Sugarcane bagasse 2%	23.67±0.11[a]	1.74±0.25[ab]	1.71±0.16[ab]	19.98
Sugarcane bagasse 3%	24.64±0.25[ab]	2.57±0.06[abcd]	2.18±0.08[ab]	20.71
Sugarcane bagasse 4%	24.19±0.09[ab]	2.47±0.63[abcd]	2.35±0.29[ab]	20.37
Sugarcane bagasse 5%	24.58±0.27[ab]	3.64±0.69[de]	3.06±0.46[ab]	20.64

All the mentioned values are means of three replicates ± standard deviation. The letters superscripted as a, b, c & d on the values shows significant differences (p < 0.05).

5.7.2.7. SEM

The Scanning electron microscopy was used to analysis the surface and cross-section of the biocomposite enforced with plant fibres. Fig. 5.11 shows the surface and cross-section of the banana pseudostems, coconut coir and sugarcane bagasse fibres based biocomposites. The addition of fibres strands can be easily visible dispersed of the surface of the composite (Simão et al., 2016). As seen in SEM micrographs in case of sugarcane bagasse fibre added composite, the surface of biocomposites are bound together within the biocomposites matrix, compactly layered with some roughness on surface indicating good dispersion (Singha et al., 2023b). The SEM micrographs show bubble free surfaced composite with presence of visible plant fibres strings. After the chemical treatment of fibres with NaOH, the process of fibrillation occurs increases the active surface area available for contact of waxy layer and intact lignocellulose components with biocomposites matrix (Otenda et al., 2022; Prasad et al., 2020; Shahi et al., 2020). In the cross-section of the biocomposites, the fibre strand was pulled out of film was noticed (Kumar and Raja, 2021). The composite also showed rough surface and presence of voids etc., and the reason responsible for voids in between the fibre and the matrix are due to improper cutting, tearing or presence of impurities (Prasad et al., 2020). Sugarcane bagasse added composite have smoother cross-section than coconut and banana fibre added biocomposites.

Banana pseudostem (surface)

Banana pseudostem (cross-section)

Coconut coir biocomposites (surface)

Coconut coir (cross-section)

Sugarcane bagasse biocomposites (surface)

Sugarcane bagasse biocomposites (cross-section)
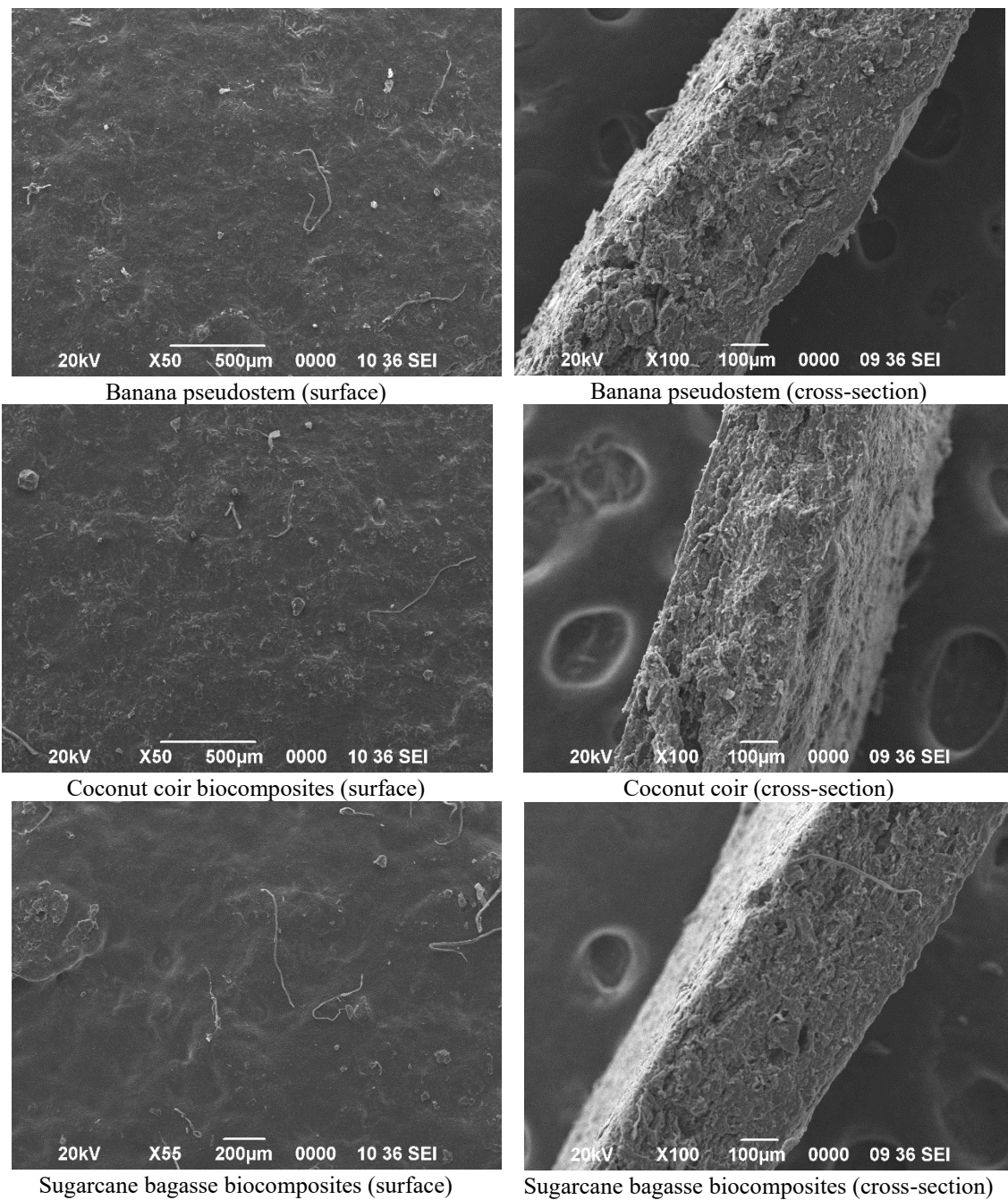
Fig. 5.11. SEM of biocomposites reinforced with plant fibres

5.7.2.8. XRD

The Crystal structures of the biocomposites were examined using X-ray diffraction (XRD). XRD pattern of banana pseudostem, coconut coir and sugarcane bagasse fibre added composite are shown in Fig. 5.12. The percentage of crystallinity index of banana pseudostem fibres, coconut coir and sugarcane bagasse fibres added biocomposites were 34.02%, 43.88% and 46.38%. The main 2θ diffraction peaks were recorded close to 14.97º, 22.4 for banana pseudostem added composite; 34.97º, 22.16º and 14.61º for coconut coir

added composite (Divyashree et al., 2016); 15.58º, 22.23º and 34.55º for sugarcane bagasse fibre added composite. Similar study was observed in Shahi et al., (2020) on film fabrication cellulose from sugarcane bagasse nanofibre extract. The 2θ diffractions were adjacent in range of 16.5º to 22.2º were associated with the presence of crystalline cellulose but sharp peaks were not observed in the graphs of the XRD due to the partially amorphous nature (Sivadas et al., 2019) indicating that type I cellulose was converted into type II cellulose and many amorphous cellulose structures were generated during ionic liquid dissolution and regeneration (Ai et al., 2021). The standard cellulose I structure, with crystalline peaks at 16.7°, 22°, and 34.08°, is present in all of the biocomposites. These peaks bear similarities to lignocellulosic source derivatives of cellulose (Jagadeesan et al., 2023).
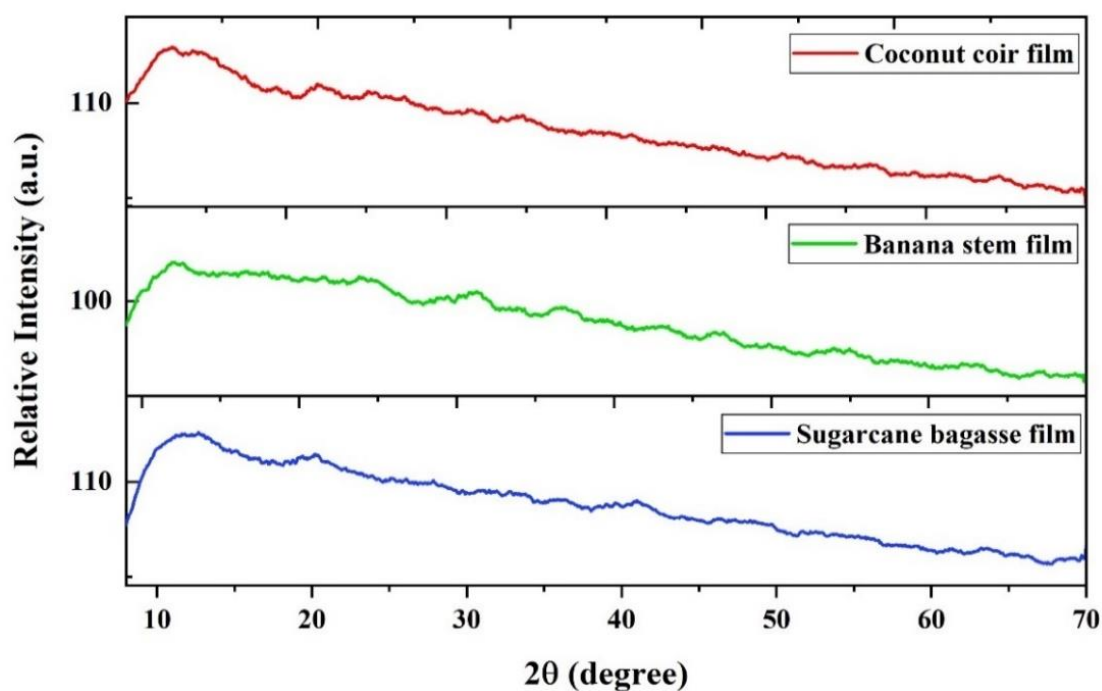
Fig. 5.12. XRD of biocomposites reinforced with plant fibres

5.7.2.9. TGA and DSC

Thermogravimetric analysis are used to study the thermal stability and degradation process of the biocomposites in a wide temperature range. The TGA curves and DTG thermograms of the banana pseudostem, coconut coir and sugarcane bagasse fibre reinforced biocomposites are presented in Fig. 5.13. TGA graph uses DTG curve to determine the charts derivative of the sample attributed to time and temperature. The degradation of the sample such as mass loss, peak temperature and mass remained after

loss are recorded after pyrolysis process of the biocomposites in presence of nitrogen gas. The major mass loss was observed in 3 stages in all the biocomposites. In the 1st stage of mass loss for banana pseudostem, coconut coir and sugarcane bagasse fibre added composite were at 31-197 °C, 47-196 °C and 37-189 °C was 7.34%, 9.13% and 9.98% respectively due to evaporation of extra bound moisture in the biocomposites. In the 2nd stage of mass loss for banana pseudostem, coconut coir and sugarcane bagasse fibre added composite were at 197-342 °C, 196-343 °C and 189-346 °C was 41.9%, 42.64% and 38.18% respectively. The wide range of mass loss is due to the decomposition of cellulose presence in fibres in biocomposites. In the 3rd stage of mass loss for banana pseudostem, coconut coir and sugarcane bagasse fibre added composite were at 342-598. °C, 343-597 °C and 346-597 °C was 11.35%, 13.97% and 10.08% respectively. The higher temperature for decomposition was due to the degradation of non-cellulosic materials in the fibres and amount of lignin present in the fibres. The residual mass left after analysis was 29.55%, 29.71% and 28.24% for banana pseudostem, coconut coir and sugarcane bagasse fibre added composite respectively.

Table 5.10 deliberates the thermal properties of the biocomposites through DSC. DSC enables the study of different thermal parameters of the plant fibres enriched biocomposites such as melting temperature (T_m), crystallization temperature (T_c), glass transition temperature (T_g), and degradation temperature (T_d). As per DSC thermograph obtained for composite, there was presence of two endothermic peaks and one exothermic peaks in all the graphs. The glass transition temperature (T_g) was obtained from the onset temperatures of 1st endothermic peaks at 75 °C, 70 °C and 67 °C for banana pseudostem, coconut coir and sugarcane bagasse fibre added composite respectively. According to DSC analysis in Fig. 5.14, it was reported that the first endothermic peak between the temperature range of 75 °C to 187 °C for banana fibre biocomposites, 70°C to 197°C for coconut coir biocomposites and 67-180°C for sugarcane bagasse fibre biocomposites represents the downward shift of the temperature after incorporation of fibres into the biocomposite matrix showing glass transition temperature of the biocomposites. The second endothermic peak range between the temperature 187°C to 285°C, 197°C to 277°C and 180°C to 280°C representing the melting temperature of banana pseudostem, coconut coir and sugarcane bagasse fibre added biocomposites respectively. The third and the last exothermic peak had small temperature range from 325°C to 372°C, 315°C to 370°C and 315 to 365°C for banana pseudostem, coconut coir and sugarcane bagasse fibre added

biocomposites respectively representing degradation of plant fibre's lignin presence in the biocomposites. The enthalpy of melting or fusion obtained for banana pseudostem added biocomposites were 6.58, 5.90 and 1.65 J/g for 1st and 2nd endothermic peaks and 3rd exothermic peaks respectively; the enthalpy of melting or fusion obtained for coconut coir added biocomposites were 50.65, 22.05 and 11.68 J/g for 1st and 2nd endothermic peaks and 3rd exothermic peaks respectively and the enthalpy of melting or fusion obtained for sugarcane bagasse fibre added biocomposites were 13.96, 7.06 and 1.94 J/g for 1st and 2nd endothermic peaks and 3rd exothermic peaks respectively (Abera et al., 2023; da Luz et al., 2018; Jagadeesan et al., 2023; Sathasivam et al., 2010; Wu et al., 2019).
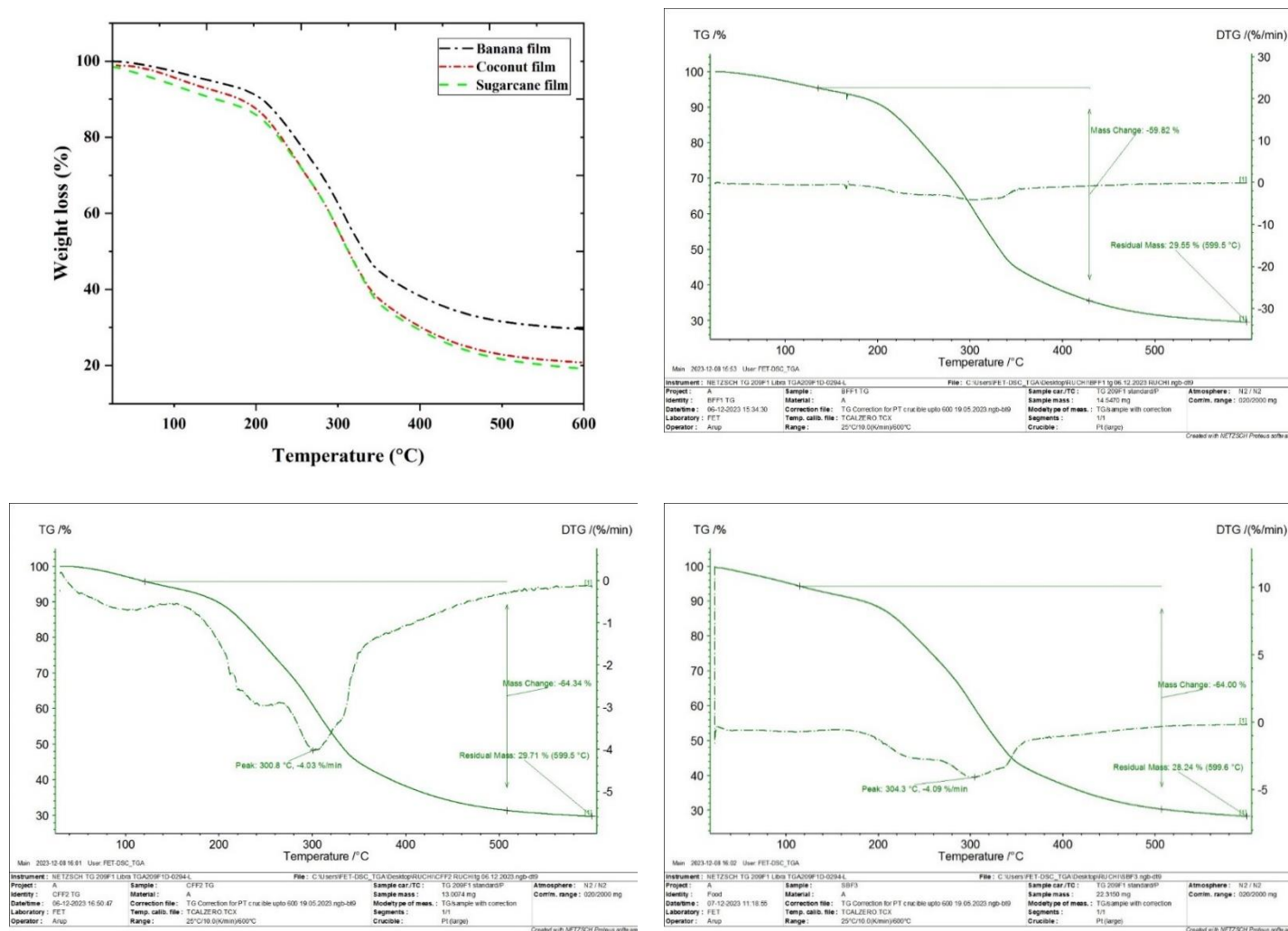
Fig. 5.13. TGA of biocomposites reinforced with plant fibres

Phase 1

Phase 2
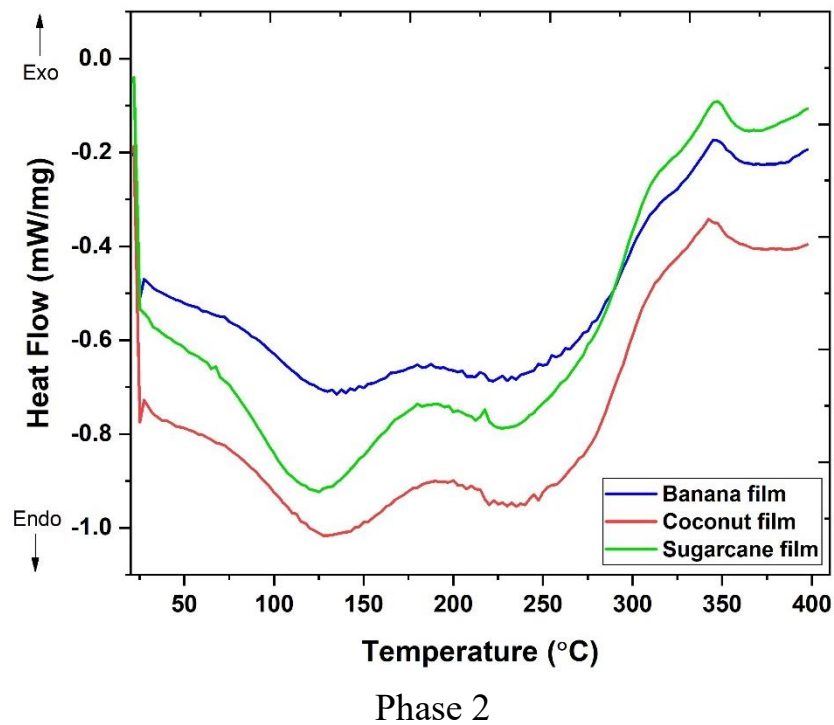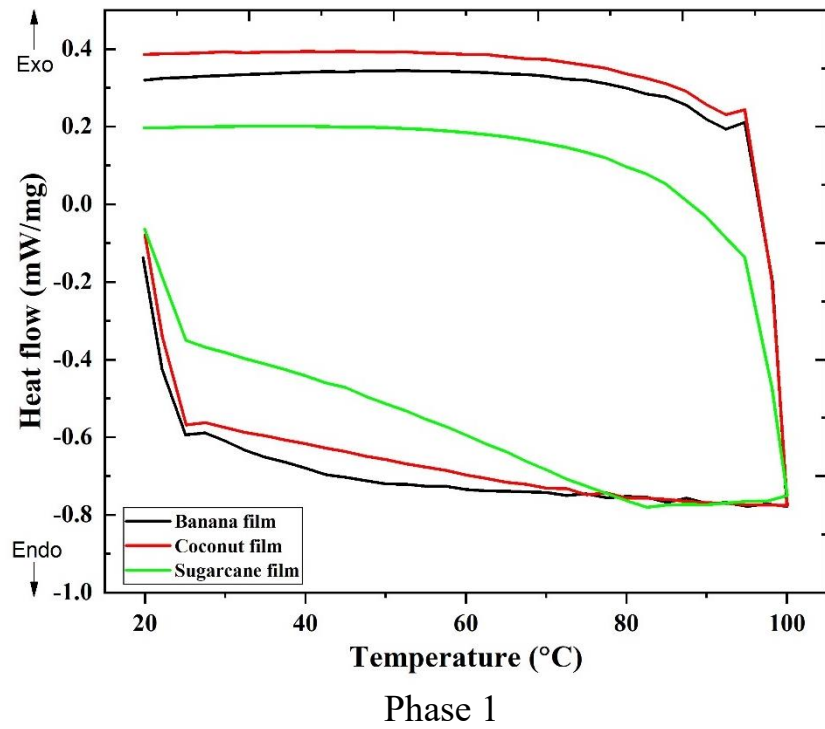
Fig. 5.14. DSC of biocomposites reinforced with plant fibres

Table 5.10. DSC of biocomposites incorporated with plant fibres

Peaks	Banana pseudostem fibre added biocomposites			Coconut coir fibre added biocomposites			Sugarcane bagasse fibre added biocomposites		
	Melting Temperature range (ºC)		Enthalpy (J/g)	Melting Temperature range (ºC)		Enthalpy (J/g)	Melting Temperature range (ºC)		Enthalpy (J/g)
	T_o	T_e	ΔH_m	T_o	T_e	ΔH_m	T_o	T_e	ΔH_m
1st endotherm	75	187	6.58	70	197	50.65	67	180	13.96
2nd endotherm	187	285	5.90	197	277	22.05	180	280	7.06
3rd exotherm	325	327	1.65	315	370	11.68	315	365	1.94

5.7.2.10. FTIR

Functional groups can be used to determine the chemical structure of any treatment (Sukyai et al., 2018). The FTIR spectra of the banana pseudostem, coconut coir and sugarcane bagasse fibre reinforced biocomposites are presented in Fig. 5.15. The common wavenumber was recorded in all the biocomposites were in range of 3427-3432 cm^{-1} of OH stretching alcohol intermolecular bond of cellulose. The spectra wavenumber obtained in between 2900-2922 cm^{-1} showing the presence of chlorophyll and 2800-3000 cm^{-1} N-H stretching of amine salt. At 2851-2854 cm^{-1} wavenumber in the graph represents the possibility of aldehydes in the biocomposites. There was presence of strong C=O stretching and OH bending of moisture in the form of water-soluble hemicellulose in range between 1733-1715 cm^{-1}. At wavenumber range 1735-1738 cm^{-1}, there was presence of formulates α, β- unsaturated ester of carboxylic stretching group of ferulic acid. The presence of cellulose symmetric deformation of CH$_2$ group was noted at 2364 cm^{-1} and 2330 cm^{-1} was presence of hemicellulose attributed to OH stretching of carbonyl group. The presence of hemicellulose in the biocomposites was clearly shown at wavenumber range 1249-1731 cm^{-1}. At 1648-1658 cm^{-1}, there was presence of C=C stretching of alkene vinylidene. The strong stretching of nitro-compound at range between 1550-1500 cm^{-1} and at 1409 cm^{-1} shows the presence of sulfonyl chloride. Both nitro-compound as well sulfonyl chloride show the presence of oilseed meals in the biocomposites. At 1443 cm^{-1} shows C-O-C bond of the cellulose chain. The presence of skeleton vibration of lignin in the biocomposites were observed by C-H asymmetric deformation, medium O-H alcohol bending, absorption associated with stretching vibrations of aromatic C=C and acetyl group of hemicellulose at recorded at wavenumber 1313-1378 cm^{-1}. At wavenumber range of 1230-1245 cm^{-1} was the presence of lignin skeleton stretching of C-O. At range 1150-1087 cm^{-1} , data showed

strong C-O stretching of aliphatic ether and at range 1040-1060 cm^{-1} showed strong broad CO-O-CO stretching anhydride and glycosidic linkage indicate high content. At wavenumber between 1030 and 1070 cm^{-1}, strong S=O sulfoxide stretching due presence of oilseed meals was observed. The symmetric in-phase stretching mode in lignin at 674 cm^{-1} and at 525 cm^{-1} showed narrow peak associated with in plane aromatic ring deformation vibration commonly for carbon presence (Divyashree et al., 2016; Gilfillan et al., 2014; Kumar and Raja, 2021; Li et al., 2015; Rosa et al., 2010; Shahi et al., 2020).
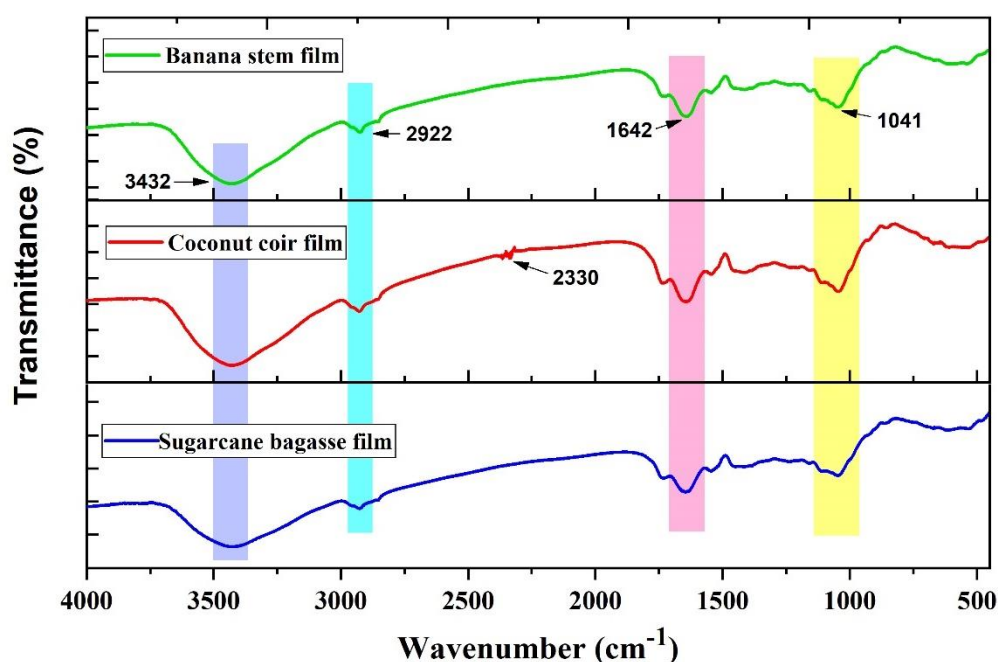
Fig. 5.15. FTIR of biocomposite reinforced with plant fibres

5.7.3. Characterization of biodegradable plates

To order to achieve the best combination of plant fibres to be used for the development of biodegradable plates, the plant fibres reinforced biocomposites were primarily developed and analysed. Through the analysis based on mechanical, barrier, physical and thermal properties, it was determined that the ideal percentage for biocomposites formulation with 5% of plant fibres (banana pseudo-stem, coconut coir and sugarcane bagasse). The developed biodegradable plates were further analyzed on the basis of physical, mechanical, color and biodegradability.

5.7.3.1. Thickness

The average thickness of the banana pseudo-stem fibre added biodegradable plates were 4.45 mm; coconut coir fibre added biodegradable plates was 4.72 mm; and sugarcane bagasse fibre added biodegradable plates was 4.07 mm. The study is in line with the result reported by Changmai and Badwaik, (2021); Ferreira et al., (2016). The thickness of the biodegradable plates is shown in Table 5.11.

5.7.3.2. Moisture content

The moisture content of the biodegradable plates is shown in Table 5.11. The moisture content of banana pseudo-stem fibre added biodegradable plates was 11.58%; coconut coir fibre added biodegradable plates was 7.28%; and sugarcane bagasse fibre added biodegradable plates was 11.68%. Less than 10% (wb) moisture content produced a stiffer, stronger sample. Higher moisture level in the samples makes them less stiff, perhaps insufficient to hold the weight of the desired product, and so less useful (Mohareb and Mittal, 2007). Similar finding were observed in the literatures of Harikrishnan et al., (2023) where the cutlery product developed from virgin coconut oiled cake and wheat bran fibre had 12.29% moisture content and virgin coconut oiled cake with gaur gum had 12.30% moisture content.

5.7.3.3. Color

The L*, a* and b* of banana pseudo-stem, coconut coir fibre and sugarcane bagasse fibre added biodegradable plates was 31.10, 32.73, 30.26; 9.16, 9.63, 8.79 and 13.66, 15.13, 12.57 respectively. The color analysis results are presented in Table 5.11. This darkness in color of the biodegradable plates were due to the dark color of the oilseed meals as raw materials and the fibres (banana pseudo-stem, coconut coir and sugarcane bagasse) added in the development of plates also imparts brown color of lignin (Kaisangsri et al., 2012).

5.7.3.4. True density

A substance's true density is determined by dividing its compressed mass by its volume without air. Finding the actual density of each component in a composite material, such as plant fibres, is crucial when choosing a material, particularly if a lightweight composite is required (Dan-Asabe et al., 2013). The true density of the biodegradable plates are presented in Table 5.11. The true density was found highest in banana pseudo-stem fibre with 0.73 g/cm^3 in comparison to coconut coir fibre (0.66 g/cm^3) and sugarcane

bagasse fibre (0.57 g/cm^3) added biodegradable plates. The density was found higher than biodegradable foam trays developed with cassava starch blended with the natural polymers of kraft fibre and chitosan with density 0.14g/cm^3 (Kaisangsri et al., 2012).

5.7.3.5. Water holding capacity

The water holding capacity or water absorption capacity of banana pseudo-stem fibre added biodegradable plates was 26.89%, coconut coir fibre added biodegradable plates was 29.82%, and sugarcane bagasse fibre added biodegradable plates was 21.69%. Similar water absorption capacity increase was noted in edible cutlery spoons developed by employing wheat flour, ragi flour, sorghum flour and Indian ginseng roots powder with 9.70% to 39.50% within 30 min (Hazra and Sontakke, 2023). The water holding capacity of the biodegradable plates are presented in Table 5.11.

Table 5.11. Physical properties and color analysis of biodegradable plates incorporated with plant fibres

Properties	BPBS	BPCC	BPSB
Moisture content (%)	11.58±0.13[b]	7.28±0.21[a]	11.68±0.20[b]
Thickness (mm)	4.45±0.32[a]	4.72±0.21[a]	4.07±0.50[a]
Water holding capacity (%)	26.89±1.59[ab]	29.82±3.03[b]	21.69±2.44[a]
True density	0.73±0.02[c]	0.66±0.01[b]	0.57±0.02[a]
L*	31.10±2.26ab	32.73±1.31b	30.26±1.24a
a*	9.16±0.50a	9.63±0.42a	8.79±0.77a
b*	13.66±1.10[ab]	15.13±0.80[b]	12.57±1.14[a]

BPBS= Biodegradable plates added with banana pseuso-stem fibres, BPCC= Biodegradable plates added with coconut coir fibres & BPSB= Biodegradable plates added with sugarcane bagasse fibres. All the mentioned values are means of three replicates ± standard deviation. The letters superscripted as a, b, c & d on the values shows significant differences (p < 0.05).

5.7.3.6. Contact angle

The micro-texture and its adhesion play an important role in the study of contact angle. The surface with water contact angle >150⁰ have low adhesion and the water drop tends to roll-off even at low tilting angle of the base whereas, surface with water contact angles <150⁰ have high adhesiveness and have anisotropic wetting property with distinct water angles. That means, higher the contact angle, higher is the water hydrophobicity (Dubey and Mohanta, 2024). The contact angle of the biocomposites are presented in Fig. 5.16 and the contact angle of the biodegradable plates are presented in Fig. 5.17. The contact angle of biocomposites incorporated with banana pseudo-stem, coconut coir and

sugarcane bagasse fibre were 41.3⁰, 36.6⁰ and 33.9⁰ respectively. The contact angle was found highest with 69.8⁰ of banana pseudo-stem fibre added biodegradable plates than coconut coir fibre added biodegradable plates with 42.8⁰, while sugarcane bagasse fibre added biodegradable plates had 49.3⁰ contact angle. The contact angle of biodegradable plates was found higher than biocomposites. There is an inverse relationship between a material's contact angle and wettability. The contact angle was found to be lower than pure bee wax (97⁰) and bee wax modified with 15% zinc stearate used as coating the surface of sweet lime pomace-based containers with polyvinyl alcohol, starch sodium and carboxy methyl cellulose constant (Changmai and Badwaik, 2021). The lower contact angle in the biodegradable plates can be due to high porosity and uneven texture without any coating on the plates.

| 41.3º | 36.6º | 33.9º |

Fig. 5.16. Contact angle of biocomposites reinforced with plant fibres

Banana pseudo-stem 69.8º   Coconut coir 42.8º   Sugarcane bagasse 49.3º
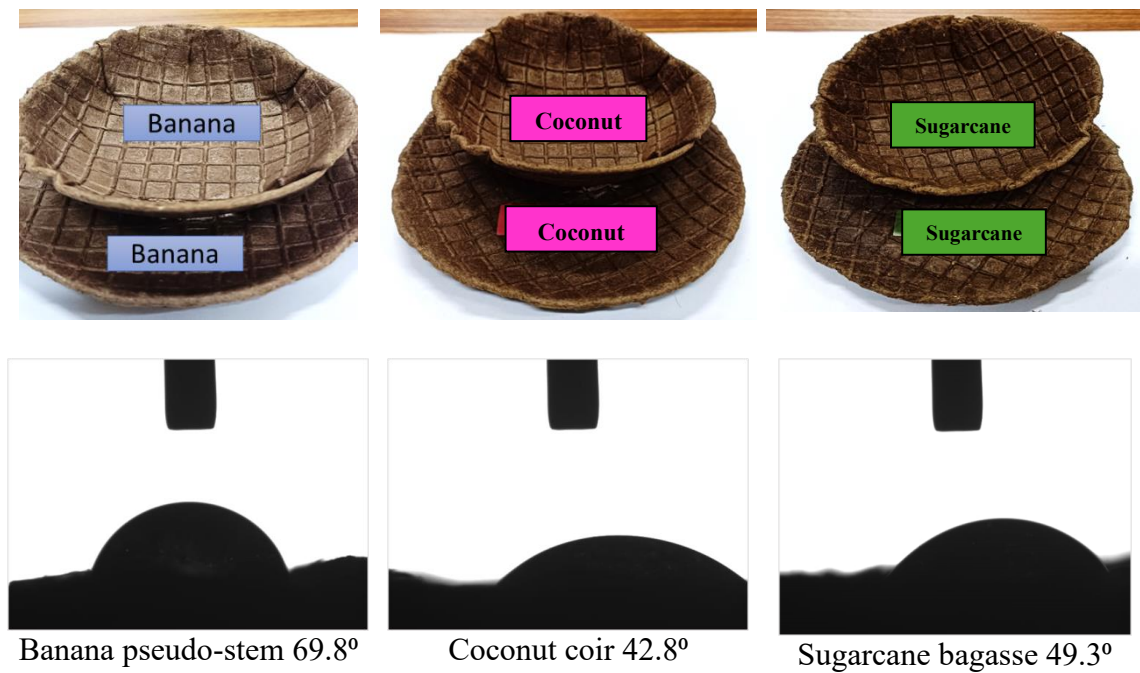
Fig. 5.17. Contact angle of biodegradable plates incorporated with plant fibres

5.7.3.7. Hardness and fracturability

The mechanical properties like hardness and fracturability was studied by compression test (at 10%, 30%, 50% and 70%) strains for the biodegradable plates. Biodegradable plates are generally hard and unbendable in structure unlike other disposable plastics and paper plates. Therefore, there was a need to test the strength and force needed to break the biodegradable plates (Rana et al., 2023). The values obtained of hardness and fracturability of the biodegradable plates are reported in Table 5.12. At 10% strain, the sugarcane bagasse had the highest fracturability value of (47.35 N) than banana pseudostem (37.58 N) and coconut coir (33.71 N) fibre based biodegradable plates whereas at 70% strain, coconut coir based biodegradable plates had the highest value of fracturability of (144.54 N) than sugarcane bagasse (129.25 N) and banana fibre (103.02 N) fibre based biodegradable plates. The hardness value at 10% strain was found the highest in banana pseudostem (84.28 N) than sugarcane bagasse (76.02 N) and coconut coir (40.05 N) whereas at 70% strain, the hardness required to break the plates was found highest in coconut coir (155.96 N) than sugarcane bagasse (144.03 N) and banana pseudostem (114.80 N) fibres based biodegradable plates. There were similar findings showing that with the addition of binder and increasing the amount of fibre in the raw material increased the samples' tensile strength. Biodegradable plates should have a higher tensile strength (Harikrishnan et al., 2023).

Table 5.12. Compression test (%) of the biodegradable plates

Biodegradable plates	Percent compression (%)	Fracturability (N)	Hardness (N)
BPBS	10	37.58±0.02	84.28±1.11
	30	82.71±0.01	84.82±0.02
	50	95.06±0.07	97.80±0.03
	70	103.02±0.02	114.80±0.08
BPCC	10	33.71±0.00	40.05±0.09
	30	34.81±0.03	61.58±0.02
	50	68.75±0.01	108.53±0.01
	70	144.54±0.05	155.96±1.51
BPSB	10	47.35±0.07	76.02±1.31
	30	67.94±1.14	105.36±0.07
	50	67.65±0.06	144.03±0.03
	70	129.25±0.03	145.93±0.04

BPBS= Biodegradable plates added with banana pseuso-stem fibres, BPCC= Biodegradable plates added with coconut coir fibres & BPSB= Biodegradable plates added with sugarcane bagasse fibres

5.7.3.8. Spreadability test

The test in performed to analyse the withholding capacity of water or different fluids in the biodegradable plates until the specified time at room temperature (Rana et al., 2023). All the plates were subjected to different food samples including water for 15 min and their results were recorded. There was no leakage, but the water was observed to spread and got absorbed more quickly than syrup when placed in all the three biodegradable plates added with banana pseudo-stem, coconut coir and sugarcane bagasse fibres within 15 min whereas, there was no spreadability observed in the plates in the presence of oil, honey or ketchup. Also, the rate of absorption was very low in the presence of oil, honey or ketchup in comparison to water within 15 min. The data recorded related to spreadability test and absorption capacity are presented in Fig. 5.18 and Table 5.13 respectively.

| Honey | Ketchup | Syrup | Oil | Water |

Fig. 5.18. Spreadability test of the biodegradable plates with different food models within 15 min

Table 5.13. Absorption capacity of the biodegradable plates with food model within 15 min

Biodegradable plates	Absorption capacity (%)
BPBS (Oil)	1.86±0.68
BPCC (Oil)	1.44±0.08
BPSB (Oil)	1.57±0.48
BPBS (Honey)	1.43±0.15
BPCC (Honey)	1.50±0.08
BPSB (Honey)	0.88±0.10
BPBS (Ketchup)	1.61±0.22
BPCC (Ketchup)	1.53±0.42
BPSB (Ketchup)	1.69±0.16
BPBS (Syrup)	1.26±0.06
BPCC (Syrup)	1.87±0.38
BPSB (Syrup)	0.79±0.13
BPBS (Water)	1.36±0.33
BPCC (Water)	3.88±1.83
BPSB (Water)	1.24±0.08

BPBS= Biodegradable plates added with banana pseuso-stem fibres, BPCC= Biodegradable plates added with coconut coir fibres & BPSB= Biodegradable plates added with sugarcane bagasse fibres

5.7.3.9. Biodegradability test

The process via which a polymer is broken down by microorganisms into biomass, carbon dioxide, water, or methane is known as biodegradation (Lucas et al., 2008). The samples were placed in the soil and humidity of the soil was maintained and the results were analysed. Each sample were weighted in every 5 days interval. The values recorded found to decrease in sample weight as shown in Fig 9. As per images, the biodegradable plates were recorded to decompose within 20 days. Since, the plates are developed from biodegradable ingredients, they started swelling and decomposing the following day and decomposed within 30 days as it was gradually seen breaking down into tiny pieces. The swelling was also seen when the plates samples taken out form soil similarly reported by Hazra and Sontakke, (2023); Rodrigues et al., (2020). The weight of the sample gradually

decreased due to the action of enzyme released by microorganisms involved in abiotic decomposition (Ferreira et al., 2020; Rodrigues et al., 2020). The biodegradation was found highest in the sugarcane bagasse incorporated plates in comparison to the banana pseudo stem and coconut coir incorporated plates. The plates were photographed in triplicate at every 5 days interval as presented in Fig. 5.19.
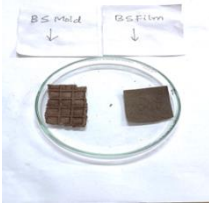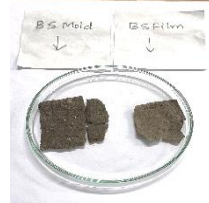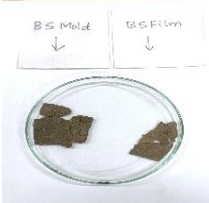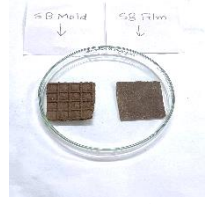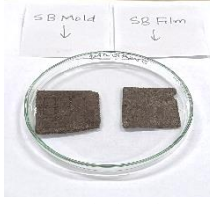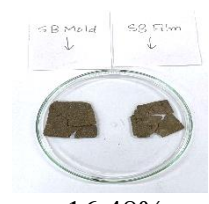

Biodegradable plates	Day 5	Day 10	Day 15	Day 20
BPBS	80.64%	60.83%	33.08%	-9.13%
BPCC	66.57%	57.55%	36.57%	-6.52%
BPSB	59.27%	56.60%	33.38%	-16.48%

Fig. 5.19. Biodegradability test of biodegradable plates reinforced with plant fibres

5.8. Conclusions

In this study, three different fibres of agricultural by-products (banana pseudo-stem, coconut coir and sugarcane bagasse) were investigated. The plant fibres were successfully extracted and studied. Cellulose, lignin and ash content was found the highest in banana pseudo-stem fibres whereas, hemicellulose was found highest in the sugarcane bagasse. Several other properties analysis in the research concluded that banana pseudo-stems, coconut coir and sugarcane bagasse had immense potential to be used in different food processing sectors instead of being wasted. The plant fibres were successfully used for the development of biocomposites and biodegradable plates

Through the characterization of biocomposites, we discovered that 5% of the plant fibres addition in the biocomposites were the best compactable for the development of biodegradable plates. An ideal biodegradable plate should have high tensile strength and low percentage elongation. The characterization of the biocomposites availed that there was decrease of moisture content and elongation at break with the addition of plant fibres but the properties like thickness, tensile strength, water vapor permeability and water solubility increased. The morphological analysis showed the surface of biocomposites had some roughness on surface indicating good dispersion. The thermal properties and % crystallinity improved with the addition of plant fibres. The FTIR analysis provided evidence of polysaccharides, proteins, chlorophyll and different components of plant fibres.

The biodegradable plates were effectively developed. The development of biocomposites generated significant benefits for selection of the amount of plant fibres addition and their compactability with oilseed meals prior to the development of biodegradable plates. The characterization of biodegradable plates, the contact angle improved in comparison to biocomposites. The biodegradable plates developed were rigid and had acceptable properties to be used as food packaging.